Division of Economics and Business
Working Paper Series

A Primer on Optimal Power Flow: Theory, Formulation, and Practical Examples

Stephen Frank
Steffen Rebennack

Working Paper 2012-14
http://econbus.mines.edu/working-papers/wp201214.pdf

Colorado School of Mines
Division of Economics and Business
1500 Illinois Street
Golden, CO 80401

October 2012

Colorado School of Mines
Division of Economics and Business
Working Paper No. **2012-14**
October 2012

Title:
A Primer on Optimal Power Flow:
Theory, Formulation, and Practical Examples*

Author(s):
Stephen Frank
Department of Electrical Engineering & Computer Science
Colorado School of Mines
Golden, CO 80401-1887
stephen.frank@ieee.org

Steffen Rebennack
Division of Economics and Business
Colorado School of Mines
Golden, CO 80401-1887
srebenna@mines.edu

ABSTRACT

The set of optimization problems in electric power systems engineering known collectively as Optimal Power Flow (OPF) is one of the most practically important and well-researched subfields of constrained nonlinear optimization. OPF has enjoyed a rich history of research, innovation, and publication since its debut five decades ago. Nevertheless, entry into OPF research is a daunting task for the uninitiated—both due to the sheer volume of literature and because OPF's familiarity within the electric power systems community has led authors to assume a great deal of prior knowledge that readers unfamiliar with electric power systems may not possess. This primer provides a practical introduction to OPF from an Operations Research perspective; it describes a complete and concise basis of knowledge for beginning OPF research. The primer is tailored for the Operations Researcher who has experience with optimization but little knowledge of Electrical Engineering. Topics include power systems modeling, the power flow equations, typical OPF formulations, and data exchange for OPF.

AMS **subject classifications: 90-01, 90C26, 90C30, 90C90**

Keywords: power flow, optimal power flow, electric power systems analysis, electrical engineering, nonlinear programming, optimization, operations research.

*This work is supported by the National Science Foundation Graduate Research Fellowship under Grant No. DGE-1057607.

1. Introduction. The set of optimization problems in electric power systems engineering known collectively as Optimal Power Flow (OPF) is one of the most practically important and well-researched subfields of constrained nonlinear optimization. In 1962, Carpentier [8] introduced OPF as an extension to the problem of optimal economic dispatch (ED) of generation in electric power systems. Carpentier's key contribution was the inclusion of the electric power flow equations in the ED formulation. Today, the defining feature of OPF remains the presence of the power flow equations in the set of equality constraints.

In general, OPF includes any optimization problem which seeks to optimize the operation of an electric power system (specifically, the generation and transmission of electricity) subject to the physical constraints imposed by electrical laws and engineering limits on the decision variables. This general framework encompasses dozens of optimization problems for power systems planning and operation [11, 36, 37]. As illustrated in Figure 1.1, OPF may be applied to decision making at nearly any planning horizon in power systems operation and control—from long-term transmission network capacity planning to minute-by-minute adjustment of real and reactive power dispatch [14, 32, 37].

To date, thousands of articles and hundreds of textbook entries have been written about OPF. In its maturation over the past five decades, OPF has served as a practical proving ground for many popular nonlinear optimization algorithms, including gradient methods [4, 10, 22], Newton-type methods [29], sequential linear programming [3, 27], sequential quadratic programming [7], and both linear and nonlinear interior point methods [15, 30, 31]. These OPF algorithms, among others, are reviewed in several surveys [17–19, 36], including one that we recently published [11, 12].

Although OPF spans both Operations Research and Electrical Engineering, the accessibility of the OPF literature is skewed heavily toward the Electrical Engineering community. Both conventional power flow (PF) and OPF have become so familiar within the electric power systems community that the recent literature assumes a great deal of prior knowledge on the part of the reader. For example, while conducting our recent survey we found that few papers even include a full OPF formulation, much less explain the particulars of the objective function or constraints. Even introductory textbooks [26, 32, 37] require a strong background in power systems analysis, specifically regarding the form, construction, and solution of the electrical power flow equations. Although many Electrical Engineers have this prior knowledge, an Operations Researcher likely will not. We believe this accessibility gap has been detrimental to the involvement of the Operations Research community in OPF research; our impression is that most OPF papers continue to be published in engineering journals by Electrical Engineers.

What is missing from the literature—and what we provide in this primer—is a practical introduction to OPF from an Operations Research perspective. The goal of this primer is to describe the tool set required to formulate, solve, and analyze a practical OPF problem. Other introductory texts for OPF focus heavily on optimization theory and tailored solution algorithms. In contrast, this primer places an emphasis on the theory and mechanics of the OPF formulation—the least documented aspect of OPF—using practical, illustrative examples.

Because we have written this primer for the Operations Researcher, we assume that the reader has significant experience with nonlinear optimization but little or no background in Electrical Engineering. Specifically, this paper requires a solid understanding of

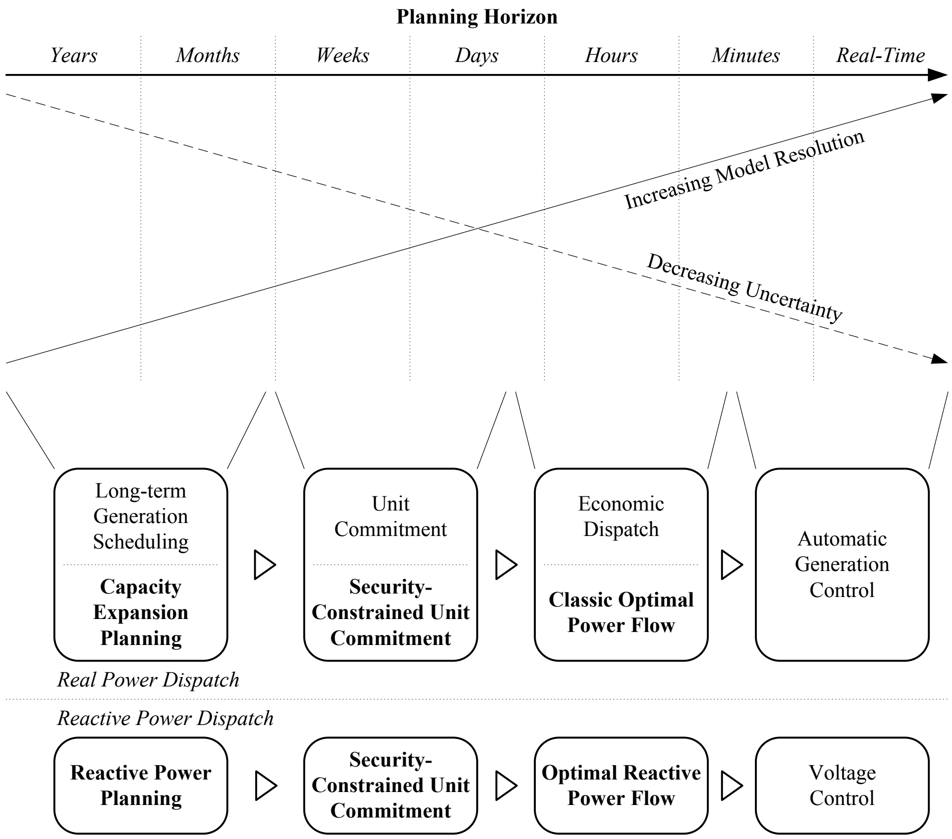

FIG. 1.1. *Optimization in power system operation via incremental planning. Long-term planning procedures make high level decisions based on coarse system models. Short-term procedures fine tune earlier decisions, using detailed models but a more limited decision space. Bold text indicates planning procedures which incorporate variants of optimal power flow.*

- linear algebra [16],
- complex number theory [13, 16],
- analysis of differential equations in the frequency domain [16], and
- linear and nonlinear optimization theory and application [20, 24].

Readers who also have a working knowledge of electrical circuits [21] and electric power systems analysis [14] will find the development of the power flow equations familiar. Other readers may wish to expand their understanding by consulting a good power systems text such as [14] or [32]. However, prior familiarity with power flow is not strictly required in order to follow the development presented in this primer.

The primer begins with a guide to OPF notation in §2, including notational differences between electric power systems engineers and Operations Researchers. Sections 3 and 4 introduce the modeling of electric power systems and the power flow equations; these fundamental topics are omitted in most other introductory OPF texts. Building upon the previous sections, §5 discusses OPF formulations; this section includes full formulations for several of the decision processes shown in Figure 1.1. §6 provides a descriptive guide to two common file formats for exchanging PF and OPF data. Finally, §7 concludes the primer.

2. Notation. In order to remain consistent with the existing body of OPF literature, this primer uses notation that follows the conventions of electric power systems engineering rather than the Operations Research community. Where there are significant differences, we have added clarifying remarks.

2.1. General. Throughout this primer, italic roman font (A) indicates a variable or parameter, bold roman font (**A**) indicates a set, and a tilde over a symbol ($\widetilde{a}$) indicates a phasor quantity (complex number). Letter case does not differentiate variables from parameters; a given quantity may be a variable in some cases and a parameter in others. Subscripts indicate indices. Symbolic superscripts are used as qualifiers to differentiate similar variables, while numeric superscripts indicate mathematical operations. For example, the superscript $^{\mathrm{L}}$ differentiates load power P^{L} from net power P, but P^2 indicates (net) power squared.

We use the following general notation for optimization formulations:

u	vector of control variables (independent decision variables)
x	vector or state variables (dependent decision variables)
ξ	vector of uncertain parameters
$f(u, x)$	objective function (scalar)
$g(u, x)$	vector function of equality constraints
$h(u, x)$	vector function of inequality constraints

The symbols e and j represent mathematical constants:

e	Euler's number (the base of the natural logarithm), $e \approx 2.71828$
j	the imaginary unit or 90° operator, $j = \sqrt{-1}$

REMARK 2.1. This differs from the common use in Operations Research of e as the unit vector and j as an index. In Electrical Engineering, j, rather than i or $\hat{\imath}$, designates the imaginary unit. For this reason, we avoid the use of j as an index throughout this primer.

In the examples, electrical units are specified where applicable using regular roman font. The unit for a quantity follows the numeric quantity and is separated by a space; for example 120 V indicates 120 Volts. The following electrical units are used in this primer:

V	Volt (unit of electrical voltage)
A	Ampere (unit of electrical current)
W	Watt (unit of real electrical power)
VA	Volt-Ampere (unit of apparent electrical power)
VAR	Volt-Ampere Reactive (unit of reactive electrical power)

2.2. Dimensions, Indices, and Sets. The following dimensions and indices are used in the OPF formulations within this primer:

N	total number of system buses (nodes)
L	total number of system branches (arcs)
M	number of system PQ buses
i, k	indices corresponding to system buses and branches
c	contingency case index
t	time period index

REMARK 2.2. We use L to indicate the number of system branches because B is reserved for the bus susceptance matrix.

REMARK 2.3. System branches are indexed as arcs between buses. For example, the branch between buses i and k is denoted by (i, k) or ik.

REMARK 2.4. In the optimization community, c typically refers to a vector of objective function coefficients. In this primer, however, we use upper case C for objective function coefficients and reserve lower case c for the contingency case index of security-constrained economic dispatch as described in §5.2.1.

There is no standard set notation within the OPF literature. (Many authors do not use sets in their formulations.) For convenience, however, we adopt the following sets in this primer:

N	set of system buses (nodes)
L	set of system branches (arcs)
M	set of load (PQ) buses
G	set of controllable generation buses
H	set of branches with controllable phase-shifting transformers
K	set of branches with controllable tap-changing transformers
Q	set of planned locations (buses) for new reactive power sources
C	set of power system contingencies for contingency analysis
T	set of time-periods for multi-period OPF

REMARK 2.5. For clarity, we use **H** and **K** to represent sets of controllable phase-shifting and tap-changing transformers rather than **S** (often used to designate sources or scenarios) and **T** (often used to designate time periods). The letters H and K otherwise have no special association with phase-shifting and tap-changing transformers.

2.3. Electrical Quantities. In power systems analysis, electrical quantities are represented in the frequency domain as phasor quantities (complex numbers). Complex numbers may be represented as a single complex variable, as two real-valued variables in rectangular form $a+jb$, or as two real-valued variables in polar form $c\angle\gamma$; all of these notations are found in the OPF literature. (Complex number notation is explained in more detail in §3.2.) Here, we document the usual symbols and relationships used for the electrical quantities; some notational exceptions exist in the literature.

2.3.1. Admittance.

$\widetilde{Z}_{ik}$	complex impedance of branch ik
R_{ik}	resistance of branch ik (real component of $\widetilde{Z}_{ik}$)
X_{ik}	reactance of branch ik (imaginary component of $\widetilde{Z}_{ik}$)
	$\widetilde{Z}_{ik} = R_{ik} + jX_{ik}$
$\widetilde{y}_{ik}$	complex series admittance of branch ik
g_{ik}	series conductance of branch ik (real component of $\widetilde{y}_{ik}$)
b_{ik}	series susceptance of branch ik (imaginary component of $\widetilde{y}_{ik}$)
	$\widetilde{y}_{ik} = 1/\widetilde{Z}_{ik} = g_{ik} + jb_{ik}$
$\widetilde{y}_{ik}^{\mathrm{Sh}}$	complex shunt admittance of branch ik
g_{ik}^{Sh}	shunt conductance of branch ik (real component of $\widetilde{y}_{ik}^{\mathrm{Sh}}$)
b_{ik}^{Sh}	shunt susceptance of branch ik (imaginary component of $\widetilde{y}_{ik}^{\mathrm{Sh}}$)
	$\widetilde{y}_{ik}^{\mathrm{Sh}} = g_{ik}^{\mathrm{Sh}} + jb_{ik}^{\mathrm{Sh}}$
$\widetilde{y}_{i}^{\mathrm{S}}$	complex shunt admittance at bus i
g_{i}^{S}	shunt conductance at bus i (real component of $\widetilde{y}_{i}^{\mathrm{S}}$)
b_{i}^{S}	shunt susceptance at bus i (imaginary component of $\widetilde{y}_{i}^{\mathrm{S}}$)
	$\widetilde{y}_{i}^{\mathrm{S}} = g_{i}^{\mathrm{S}} + jb_{i}^{\mathrm{S}}$
$\widetilde{Y}_{ik}$	complex ik^{th} element of the bus admittance matrix
Y_{ik}	magnitude of ik^{th} element of the bus admittance matrix
θ_{ik}	angle of ik^{th} element of the bus admittance matrix
G_{ik}	conductance of ik^{th} element of the bus admittance matrix (real component of

$\widetilde{Y}_{ik}$)
B_{ik} susceptance of ik^{th} element of the bus admittance matrix (imaginary component of $\widetilde{Y}_{ik}$)
$\widetilde{Y}_{ik} = Y_{ik}\angle\theta_{ik} = G_{ik} + jB_{ik}$

REMARK 2.6. Note the distinction between lowercase y, g, and b and uppercase Y, G, and B: the former represents the values corresponding to individual system branch elements, while the latter refers to the admittance matrix which models the interaction of all system branches.

2.3.2. Voltage.

$\widetilde{V}_i$ complex (phasor) voltage at bus i
V_i voltage magnitude at bus i
δ_i voltage angle at bus i
E_i real component of complex voltage at bus i
F_i imaginary component of complex voltage at bus i
$\widetilde{V}_i = V_i\angle\delta_i = E_i + jF_i$

2.3.3. Current.

$\widetilde{I}_i$ complex (phasor) current injected at bus i
I_i magnitude of current injected at bus i
$\widetilde{I}_{ik}$ complex (phasor) current in branch ik, directed from bus i to bus k
I_{ik} magnitude of current in branch ik

2.3.4. Power.

P_i^{L} load (demand) real power at bus i
Q_i^{L} load (demand) reactive power at bus i
S_i^{L} load (demand) complex power at bus i
$S_i^{\text{L}} = P_i^{\text{L}} + jQ_i^{\text{L}}$
P_i^{G} generator (supply) real power at bus i
Q_i^{G} generator (supply) reactive power at bus i
S_i^{G} generator (supply) complex power at bus i
$S_i^{\text{G}} = P_i^{\text{G}} + jQ_i^{\text{G}}$
P_i net real power injection at bus i ($P_i = P_i^{\text{G}} - P_i^{\text{L}}$)
Q_i net reactive power injection at bus i ($Q_i = Q_i^{\text{G}} - Q_i^{\text{L}}$)
S_i net complex power injection at bus i
$S_i = S_i^{\text{G}} - S_i^{\text{L}} = P_i + jQ_i$

REMARK 2.7. The phasor indicator $\widetilde{\ }$ is omitted for complex power S, as S is always understood to be a complex quantity. In the literature, the indicator $\widetilde{\ }$ is also often omitted for V, I, y, and Y, but we include it here to disambiguate the complex quantities from their associated (real-valued) magnitudes.

2.3.5. Other.

φ_{ik} phase shift of phase-shifting transformer in branch ik
T_{ik} tap ratio of tap-changing transformer in branch ik

3. Fundamental Concepts. Scholarly literature discussing OPF assumes a working knowledge of power systems models and electrical concepts, many of which may be unfamiliar to the Operations Researcher. In this section, we summarize several fundamental concepts required for power systems analysis and the development of the power flow equations as presented in §4.

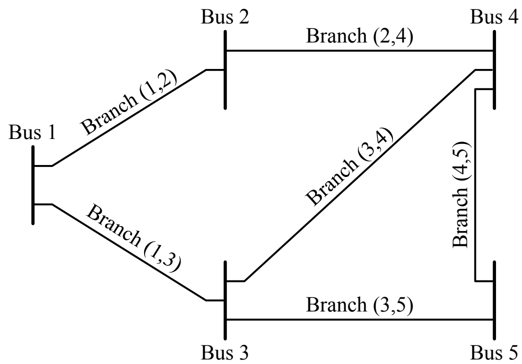

FIG. 3.1. *Bus and branch indices in an example 5-bus electrical network.*

3.1. System Representation. Electric power systems are modeled as a network of electrical nodes (buses) interconnected via admittances (branches) that represent transmission lines, cables, transformers, and similar power systems equipment. Buses are referenced by node with index $i \in \mathbf{N}$, while branches are referenced as arcs between nodes $(i, k) \in \mathbf{L}$, where $i, k \in \mathbf{N}$.

EXAMPLE 3.1. *The network in Figure 3.1 has* $N = 5$ *buses and* $L = 6$ *branches, with corresponding sets*

$$\mathbf{N} = \{1, 2, 3, 4, 5\}$$

and

$$\mathbf{L} = \{(1, 2), (1, 3), (2, 4), (3, 4), (3, 5), (4, 5)\}.$$

□

For power flow analysis, the electric power system is analyzed in the frequency domain under the assumption of sinusoidal steady-state operation. At sinusoidal steady-state, all voltage and current waveforms are sinusoids with fixed magnitude, frequency, and phase shift, and all system impedances are fixed. Under these conditions, the differential equations governing power system operation reduce to a set of complex algebraic equations involving the *phasor* representation of the system electrical quantities. This algebraic representation is much easier to solve.

3.2. Phasor Quantities. Steady-state sinusoidal voltages and currents can be fully characterized by their magnitude and phase shift using phasors. A phasor transforms a sinusoidal time-domain signal into a complex exponential in the frequency domain, using the relationship

$$\underset{\textit{Time Domain}}{c \sin(2\pi f t + \gamma)} \quad \longleftrightarrow \quad \underset{\textit{Frequency Domain}}{c e^{j\gamma}}$$

The frequency f of the signal is fixed and therefore omitted from the phasor notation. The phasor $ce^{j\gamma}$ may be written as $c\angle\gamma$ in polar coordinates or as $a + jb$ in rectangular coordinates, where, according to Euler's formula,

$$\begin{aligned} a &= c\cos\gamma, \\ b &= c\sin\gamma, \\ c &= \sqrt{a^2+b^2}, \\ \gamma &= \arctan\frac{b}{a}. \end{aligned}$$

Freitag and Busam [13] provide an overview of complex number theory, while O'Malley [21, Ch. 11] discusses the use of phasor quantities in Electrical Engineering.

Remark 3.2. In Electrical Engineering, voltage and current phasors are expressed as root-mean-square (RMS) quantities rather than peak quantities. This is done so that frequency domain power calculations yield the correct values without the need for an additional scaling factor. For a sinusoid, the RMS magnitude is $1/\sqrt{2}$ times the peak magnitude. Thus, in Electrical Engineering, a time-domain voltage waveform

$$V_{\mathrm{Pk}}\sin\left(2\pi f t+\delta\right)$$

has the frequency domain phasor

$$\frac{V_{\mathrm{Pk}}}{\sqrt{2}}e^{j\delta}.$$

Example 3.3. *The time domain voltage waveform*

$$120\sqrt{2}\sin(377t-30^{\circ})\ \mathrm{V}$$

represents the standard outlet voltage in the United States with the angle referenced, for instance, to the high side of a utility distribution transformer. This voltage has the frequency domain phasor

$$\widetilde{V} = 120e^{-j30^{\circ}}\ \mathrm{V}.$$

In polar coordinates, this phasor is

$$\widetilde{V} = 120\angle{-30^{\circ}}\ \mathrm{V},$$

while in rectangular coordinates it is

$$\begin{aligned} \widetilde{V} &= 120\cos -30^{\circ} + j120\sin -30^{\circ}\ \mathrm{V}, \\ &\approx 103.9 - j60.0\ \mathrm{V}. \end{aligned}$$

Note that the RMS voltage magnitude of 120 V *is the familiar quantity.* □

3.3. Complex Power. The product of voltage and current is electrical power. In AC power systems, however, instantaneous electrical power fluctuates as the voltage and current magnitudes change over time. For frequency domain analysis, power systems engineers use the concept of *complex power* to characterize these time domain power fluctuations.

Complex power is a phasor quantity consisting of *real power* and *reactive power*. Real power represents real work, that is, a net transfer of energy from source to load.

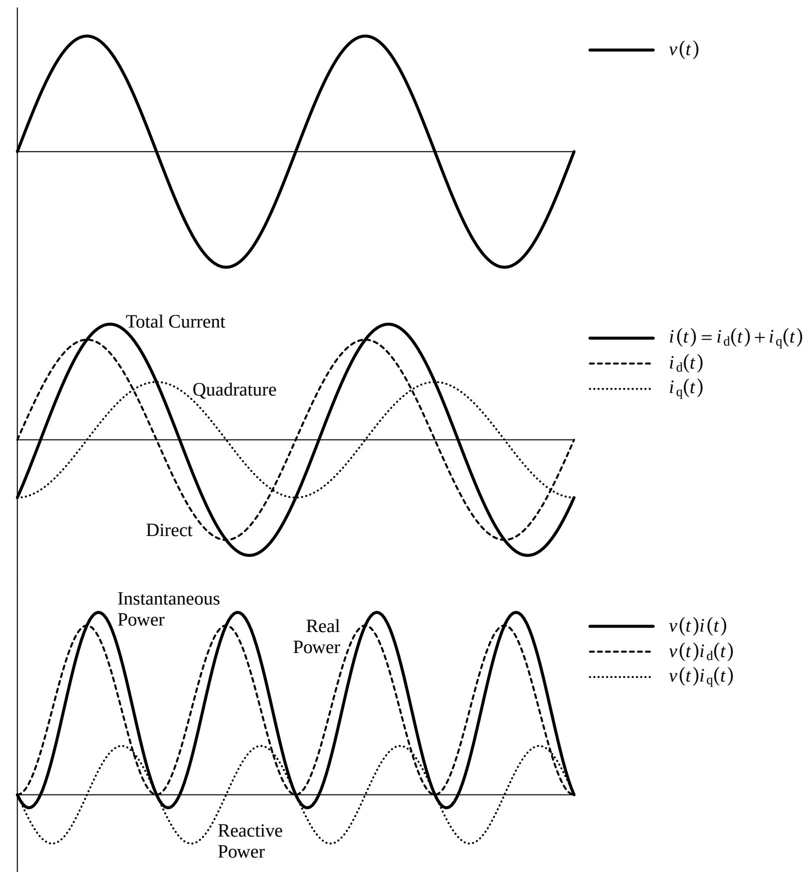

FIG. 3.2. *Conceptual illustration of real and reactive power using time domain waveforms. In the figure, current $i(t)$ lags voltage $v(t)$ by 30°.*

Reactive power, on the other hand, represents circulating energy—an cyclic exchange of energy that averages zero net energy transfer over time.

Real power transfer occurs when voltage and current are in phase, while reactive power transfer occurs when voltage and current are 90° out of phase (that is, orthogonal). An arbitrary AC current $i(t)$ can be represented by the sum of direct current $i_d(t)$ (in phase with the voltage) and quadrature current $i_q(t)$ (orthogonal to the voltage). Direct current produces real power and quadrature current reactive power, as illustrated in Figure 3.2.

By convention, reactive power is considered positive when current lags voltage. Therefore, complex power S can be computed from[1]

$$S = \widetilde{V}\widetilde{I}^* = P + jQ$$

and consists of orthogonal components P (real power) and Q (reactive power). The magnitude of complex power, $|S|$, is called the *apparent power* and is often used to specify power systems equipment and transmission line ratings. Complex and

[1] Here and elsewhere in this primer, the symbol * denotes complex conjugation rather than an optimal value. This use is typical in Electrical Engineering and consistent with most OPF literature.

apparent power have units of Volt-Amperes (VA), real power has units of Watts (W), and reactive power has units of Volt-Amperes Reactive (VAR).

REMARK 3.4. Reactive power is sometimes called imaginary power, both because it does not perform real work and because it is the imaginary part of S.

EXAMPLE 3.5. *A small electrical appliance draws* 2 $\text{A}\angle{-30^\circ}$ *from a* 120 $\text{V}\angle 0^\circ$ *source. The complex power draw of the appliance is*

$$\begin{aligned} S &= \left(120\ \text{V}\angle 0^\circ\right)\left(2\ \text{A}\angle{-30^\circ}\right)^*, \\ &= \left(120\ \text{V}\cdot 2\ \text{A}\right)\angle\left(0^\circ + 30^\circ\right), \\ &= 240\ \text{VA}\ \angle 30^\circ, \\ &\approx 207.8\ \text{W} + j120\ \text{VAR}. \end{aligned}$$

The apparent power draw of the appliance is 240 VA*, the real power is* 207.8 W*, and the reactive power is* 120 VAR*.*

We can verify that the real power is correct by examining the average power in the time domain. The voltage and current waveforms are

$$\begin{aligned} v(t) &= 120\sqrt{2}\sin(377t)\ \text{V}, \\ i(t) &= 2\sqrt{2}\sin(377t - 30^\circ)\ \text{A}, \end{aligned}$$

respectively. The instantaneous power is

$$p(t) = v(t)i(t) = 480\sin(377t)\sin(377t - 30^\circ)\ \text{W}.$$

Or, by using trigonometric identities,

$$p(t) = 240\cos(30^\circ) - 240\cos\left(2\left(377t\right) - 30^\circ\right)\ \text{W}.$$

Over time, the average power is

$$\begin{aligned} p_{\text{Avg}} &= \int_0^{\frac{1}{60}} 240\cos(30^\circ) - 240\cos\left(2\left(377t\right) - 30^\circ\right) dt\ \text{W}, \\ &= 240\cos(30^\circ) \approx 207.8\ \text{W}, \end{aligned}$$

which is identical to the real power P computed in the frequency domain. □

Both real and reactive power affect power systems operation and are therefore modeled in PF and OPF. O'Malley [21, Ch. 15] and other introductory circuits texts provide a more complete overview of complex power.

3.4. The Per-Unit System. Electric power systems quantities are usually expressed as a ratio of the actual quantity to a reference, or base, quantity; this practice is called the *per-unit* system. Per-unit quantities are unitless and are labeled using a designation, if any, of "p.u.". Nearly all OPF literature assumes a working knowledge of per-unit on the part of the reader, but this assumption is rarely stated explicitly. Indeed, power systems texts frequently mix per-unit and SI (metric) units, for instance, reporting voltage in per-unit and power in MW. As a result, per-unit can be a significant source of confusion when working with practical OPF formulations.

In power systems analysis, base quantities are given in the SI system (Volts, Amperes, Watts, Ohms, etc.), while per-unit quantities are dimensionless. The per-unit value of an SI quantity x on a given base x_{Base} is

$$x_{\text{pu}} = \frac{x}{x_{\text{Base}}}.$$

Correct interpretation of the SI value of a per-unit quantity requires knowledge of the base quantity. For example, a power of 0.15 p.u. on a 10 MVA base is equal to 1.5 MW, but 0.15 p.u. on a 1000 MVA base is equal to 150 MW.[2] All calculations that can be performed in the SI system can also be performed in per-unit. However, (i) per-unit and SI quantities cannot be mixed in calculations, and (ii) all per-unit calculations must be performed on a consistent set of bases.

With a proper selection of system bases, the per-unit system has several advantages over the SI system of measurement, most notably

1. The use of per-unit eliminates the need to distinguish between single-phase and three-phase electrical quantities;
2. The use of per-unit eliminates the need to apply voltage and current scaling factors at the majority of system transformers;
3. The use of per-unit automatically adjusts for the phase shift of three-phase transformers (Wye-Delta or Delta-Wye);
4. Per-unit quantities have consistent magnitudes on the order of 1.0, which improves the numerical stability of power flow calculations; and
5. The per-unit system is easier to interpret at a glance. (For example, per-unit voltage should always lie within the approximate range 0.95–1.05 p.u., regardless of the SI voltage.)

Once two system bases are specified, the others are fixed exactly. In power flow analysis, the voltage and power bases are specified,

$$\begin{aligned} V_{\text{Base}} &= \text{Line-to-line Voltage}, \\ S_{\text{Base}} &= \text{Three-phase Power}, \end{aligned}$$

and the remaining three-phase system bases are calculated according to

$$\begin{aligned} I_{\text{Base}} &= \frac{S_{\text{Base}}}{\sqrt{3}\ V_{\text{Base}}}, \\ Z_{\text{Base}} &= \frac{V_{\text{Base}}}{\sqrt{3}\ I_{\text{Base}}} = \frac{V_{\text{Base}}^2}{S_{\text{Base}}}, \\ Y_{\text{Base}} &= \frac{\sqrt{3}\ I_{\text{Base}}}{V_{\text{Base}}} = \frac{S_{\text{Base}}}{V_{\text{Base}}^2} = \frac{1}{Z_{\text{Base}}}. \end{aligned}$$

S_{Base} is constant throughout the power system, but V_{Base} is distinct for each system bus. For mathematical convenience, power systems engineers typically set S_{Base} to one of 10, 100, or 1000 MVA and select V_{Base} as the nominal line-to-line voltage at each bus. When V_{Base} is selected in this way, the voltage ratio of most system transformers becomes 1:1 in per-unit, simplifying the development of the system admittance matrix; see §4.1.

Example 3.6. *12.47 kV is a common distribution voltage level in the United States. If a nominally* 12.47 kV *feeder is operated at 0.95 p.u., then its voltage level in SI units is*

$$\begin{aligned} V_{\text{SI}} &= 0.95 \cdot 12.47 \text{ kV}, \\ &= 11.85 \text{ kV}. \end{aligned}$$

[2] In per-unit, real power (W), reactive power (VAR), and apparent power (VA) share a common base with units of VA.

Similarly, a nominally 12.47 kV *feeder operating at* 13.2 kV *(another common distribution voltage level) has a per-unit voltage of*

$$\begin{aligned} V_{\text{pu}} &= \frac{13.2 \text{ kV}}{12.47 \text{ kV}}, \\ &= 1.059 \text{ p.u.} \end{aligned}$$

□

In OPF, a common convention is to specify source and load power in SI units, indicate the system power base, and specify all other quantities directly in per-unit; see §6. The power values must be converted to per-unit prior to evaluating the power flow equations, but usually no other conversions are necessary. Glover, Sarma, and Overbye [14] provide additional discussion of the per-unit system, including instructions for base conversions, relationships for single-phase bases, and practical examples.

4. The Power Flow Equations. In this section, we develop the power flow equations and present the mechanics of their construction. The steady-state operation of an alternating current (AC) electrical network is governed by the matrix equation

$$\widetilde{I} = \widetilde{Y}\widetilde{V} \tag{4.1}$$

where

$$\widetilde{I} = \left(\widetilde{I}_1, \ldots, \widetilde{I}_N\right)$$

is an N-dimensional vector of phasor currents injected at each system bus,

$$\widetilde{V} = \left(\widetilde{V}_1, \ldots, \widetilde{V}_N\right)$$

is an N-dimension vector of phasor voltages at each system bus, and

$$\widetilde{Y} = \begin{pmatrix} \widetilde{Y}_{11} & \ldots & \widetilde{Y}_{1N} \\ \vdots & \ddots & \vdots \\ \widetilde{Y}_{N1} & \ldots & \widetilde{Y}_{NN} \end{pmatrix}$$

is the $N \times N$ complex bus admittance matrix. In practical power systems, $\widetilde{I}$ represents the current supplied by generators and demanded by loads, while $\widetilde{Y}$ models transmission lines, cables, and transformers. Traditionally, the elements of $\widetilde{Y}$ were considered constant, but in newer OPF formulations $\widetilde{Y}$ may contain both constants and control (decision) variables. The voltages $\widetilde{V}$ are state variables which fully characterize the system operation for a given matrix $\widetilde{Y}$.

In power systems analysis, it is more convenient to work with power flows than currents because (i) injected powers are independent of system voltage angle while injected currents are not, and (ii) working directly with power allows straightforward computation of required electrical energy. Therefore, power systems engineers transform (4.1) into the complex power flow equation

$$S = \widetilde{V} \circ \left(\widetilde{Y}\widetilde{V}\right)^*, \tag{4.2}$$

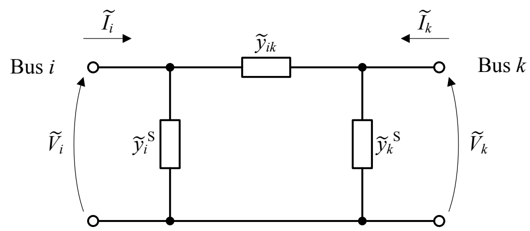

FIG. 4.1. *Example two-bus network illustrating the definitions of bus voltage and injected current.*

where $S = P + jQ$ is a vector of complex power injections at each bus and $\circ$ denotes element-wise vector multiplication. At each bus, the total injected power is the difference between the generation and the load,

$$S_i = S_i^{\mathrm{G}} - S_i^{\mathrm{L}},$$
$$P_i = P_i^{\mathrm{G}} - P_i^{\mathrm{L}},$$
$$Q_i = Q_i^{\mathrm{G}} - Q_i^{\mathrm{L}}.$$

Typically, load real and reactive power are fixed while generation real and reactive power are control variables with minimum and maximum limits.

4.1. The Admittance Matrix. The bus admittance matrix $\widetilde{Y}$ forms the core of the power flow equations. OPF data generally does not give $\widetilde{Y}$ directly, and therefore we summarize the mechanics of its construction here. The elements of $\widetilde{Y}$ are derived from the application of Ohm's law, Kirchoff's current law (KCL), and Kirchoff's voltage law (KVL) to a steady-state AC electrical network; O'Malley [21] provides a concise summary of these electrical laws. At each bus i, $\widetilde{I}_i$ is the net current flowing out of the bus through all connected branches, that is, the current injected from outside sources (such as connected generators or loads) required to satisfy KCL. From Ohm's law and KVL,

$$\widetilde{I}_i = \widetilde{V}_i \widetilde{y}_i^{\mathrm{S,Total}} + \sum_{k:(i,k)\in\mathbf{L}} \left(\widetilde{V}_i - \widetilde{V}_k\right) \widetilde{y}_{ik} + \sum_{k:(k,i)\in\mathbf{L}} \left(\widetilde{V}_i - \widetilde{V}_k\right) \widetilde{y}_{ki} \tag{4.3}$$

where $\widetilde{y}_{ik}$ is the admittance of branch (i,k) and $\widetilde{y}_i^{\mathrm{S,Total}}$ is the total shunt admittance from bus i to neutral. In matrix form, (4.1) is equivalent to (4.3) when the elements of $\widetilde{Y}$ are defined as

$$\begin{aligned} \widetilde{Y}_{ii} &= \sum \text{Admittances directly connected to bus } i \\ \widetilde{Y}_{ik} &= -\sum \text{Admittances directly connected between bus } i \text{ and bus } k \end{aligned} \tag{4.4}$$

Typically, only a single branch (i,k) connects bus i to bus k, in which case the off-diagonal elements become $\widetilde{Y}_{ik} = \widetilde{Y}_{ki} = -\widetilde{y}_{ik}$. If there is no connection between buses i and k, $\widetilde{Y}_{ik} = 0$. Thus, $\widetilde{Y}$ is sparse, having dimension $N \times N$ but only $N + 2L$ nonzero entries. In this section, we first document the types of branch elements used in power flow analysis and then develop a general expression for the entries of $\widetilde{Y}$ that satisfies (4.4).

EXAMPLE 4.1. *Figure 4.1 shows an example network consisting of two buses i and k and a single branch (i,k) between them. Branch (i,k) has series admittance*

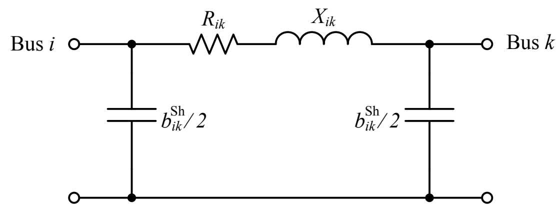

FIG. 4.2. Π *branch model for cables and transmission lines.*

$\widetilde{y}_{ik}$*, and each bus also has a shunt admittance. For this network, writing* (4.3) *for each bus yields the matrix equation*

$$\begin{pmatrix} \widetilde{I}_i \\ \widetilde{I}_k \end{pmatrix} = \begin{pmatrix} \widetilde{y}_{ik} + \widetilde{y}_i^{\text{S}} & -\widetilde{y}_{ik} \\ -\widetilde{y}_{ik} & \widetilde{y}_{ik} + \widetilde{y}_k^{\text{S}} \end{pmatrix} \begin{pmatrix} \widetilde{V}_i \\ \widetilde{V}_k \end{pmatrix}.$$

□

4.1.1. Cables and Transmission Lines. Power cables and transmission lines are modeled as Π branch circuits (Figure 4.2). The line characteristics are specified as a series impedance $R_{ik} + jX_{ik}$ and a branch shunt admittance jb_{ik}^{Sh}, which is sometimes given as "line charging" reactive power. The Π branch series admittance $\widetilde{y}_{ik}$ for inclusion in $\widetilde{Y}$ is

$$\widetilde{y}_{ik} = \frac{1}{R_{ik} + jX_{ik}} = \frac{R_{ik}}{R_{ik}^2 + X_{ik}^2} - j\frac{X_{ik}}{R_{ik}^2 + X_{ik}^2}, \tag{4.5}$$

$$g_{ik} = \frac{R_{ik}}{R_{ik}^2 + X_{ik}^2},$$

$$b_{ik} = \frac{R_{ik}}{R_{ik}^2 + X_{ik}^2}.$$

Branch shunt susceptance b_{ik}^{Sh} is related to but distinct from the net shunt susceptance at buses i and k. Specifically, the branch shunt susceptance b_{ik}^{Sh} is divided into two equal parts and added to bus shunt susceptances b_i^{S} and b_k^{S} at each end of the line, as illustrated in Figure 4.2. For short lines, branch shunt susceptance is usually omitted.

4.1.2. Transformers. Most power systems transformers have nominal turns ratios, that is, the voltage ratio across the transformer exactly equals change in system voltage base across the transformer (a 1:1 voltage ratio in per-unit, with no phase shift). Because the per-unit system automatically accounts for the turns ratio, the branch model for a transformer with nominal turns ratios is identical to the Π branch circuit for a transmission line (Figure 4.2). However, in power flow analysis, transformer branches are almost always modeled with zero shunt susceptance and often with zero series resistance as well.

4.1.3. Off-Nominal Transformers. Any transformer that does not have exactly a 1:1 voltage ratio in per-unit is an off-nominal transformer. This category includes fixed-tap transformers with off-nominal turns ratios, tap-changing transformers, and phase-shifting transformers. Off-nominal transformers require modified entries in $\widetilde{Y}$ to account for the additional voltage magnitude or phase angle change relative to the nominal case. Proper modeling of off-nominal transformers is a key

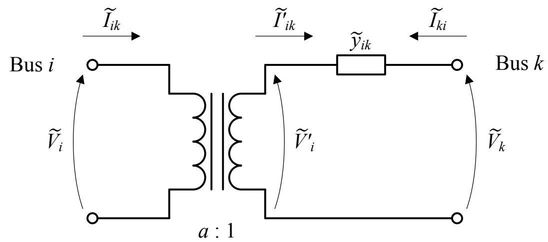

FIG. 4.3. *Off-nominal transformer branch model.*

skill in developing practical OPF algorithms. Unfortunately, this topic is neglected in most introductory OPF texts.

Figure 4.3 displays the standard model for off-nominal transformers found in practical power flow and OPF software. In the model, bus i is the *tap bus* and bus k is the *impedance bus* or *Z bus*. The transformer turns ratio in per-unit is a:1, where a is a complex exponential consisting of magnitude T and phase shift φ,

$$a = Te^{j\varphi},$$

such that $\widetilde{V}_i = a\widetilde{V}_i'$ and $\widetilde{I}_{ik} = \widetilde{I}'_{ik}/a^*$. Selecting $T = 1$ and $\varphi = 0$ yields the nominal turns ratio. In OPF, either T or φ (or both) may be a control variable: controllable T models an on-load tap changer, while controllable φ models a phase shifting transformer.

In order to include the effects of off-nominal transformer (i, k) in $\widetilde{Y}$, partial admittance matrix entries for branch (i, k) are required such that

$$\begin{pmatrix} \widetilde{I}_{ik} \\ \widetilde{I}_{ki} \end{pmatrix} = \begin{pmatrix} \widetilde{Y}'_{ii} & \widetilde{Y}'_{ik} \\ \widetilde{Y}'_{ki} & \widetilde{Y}'_{kk} \end{pmatrix} \begin{pmatrix} \widetilde{V}_i \\ \widetilde{V}_k \end{pmatrix}.$$

Using the turns ratio definitions given above and Ohm's law, the expression for current $\widetilde{I}_{ik}$ is developed as follows:

$$\begin{aligned} \widetilde{I}_{ik} &= \frac{1}{a^*}\widetilde{I}'_{ik}, \\ &= \frac{1}{a^*}\widetilde{y}_{ik}\left(\widetilde{V}_i' - \widetilde{V}_k\right), \\ &= \frac{1}{a^*}\widetilde{y}_{ik}\left(\frac{1}{a}\widetilde{V}_i - \widetilde{V}_k\right), \\ &= \frac{1}{aa^*}\widetilde{y}_{ik}\widetilde{V}_i - \frac{1}{a^*}\widetilde{y}_{ik}\widetilde{V}_k. \end{aligned} \tag{4.6}$$

Similarly,

$$\begin{aligned} \widetilde{I}_{ki} &= \widetilde{y}_{ik}\left(\widetilde{V}_k - \widetilde{V}_i'\right), \\ &= \widetilde{y}_{ik}\left(\widetilde{V}_k - \frac{1}{a}\widetilde{V}_i\right), \\ &= -\frac{1}{a}\widetilde{y}_{ik}\widetilde{V}_i + \widetilde{y}_{ik}\widetilde{V}_k. \end{aligned} \tag{4.7}$$

In matrix form, expressions (4.6) and (4.7) become

$$\begin{pmatrix} \widetilde{I}_{ik} \\ \widetilde{I}_{ki} \end{pmatrix} = \begin{pmatrix} \frac{1}{aa^*}\widetilde{y}_{ik} & -\frac{1}{a^*}\widetilde{y}_{ik} \\ -\frac{1}{a}\widetilde{y}_{ik} & \widetilde{y}_{ik} \end{pmatrix} \begin{pmatrix} \widetilde{V}_i \\ \widetilde{V}_k \end{pmatrix}. \tag{4.8}$$

The differing expressions for $\widetilde{I}_{ik}$ and $\widetilde{I}_{ki}$ in (4.8) indicate the importance of the difference between the tap bus i and the Z bus k; reversing the two leads to considerable error.

When constructing the full admittance matrix $\widetilde{Y}$, the relationships of (4.8) must be preserved. If $\widetilde{Y}$ has previously been constructed according to (4.4) with off-nominal voltage ratios neglected, then the following correction procedure is required for each off-nominal branch (i,k):

1. The partial diagonal term corresponding to branch (i,k) in $\widetilde{Y}_{ii}$ is divided by $aa^* = |a|^2$, as given by the replacement procedure

$$\widetilde{Y}_{ii} \longleftarrow \widetilde{Y}_{ii}^{Old} - \widetilde{y}_{ik} + \frac{1}{aa^*}\widetilde{y}_{ik},$$

where $\widetilde{y}_{ik}$ is the uncorrected partial diagonal admittance term.

2. The partial diagonal admittance term corresponding to branch (i,k) in $\widetilde{Y}_{kk}$ remains unchanged.

3. The off-diagonal admittance matrix entry $\widetilde{Y}_{ik}$ is divided by a^*, as given by the replacement procedure

$$\widetilde{Y}_{ik} \longleftarrow -\frac{1}{a^*}\widetilde{y}_{ik}.$$

4. The off-diagonal admittance matrix entry $\widetilde{Y}_{ki}$ is divided by a, as given by the replacement procedure

$$\widetilde{Y}_{ki} \longleftarrow -\frac{1}{a}\widetilde{y}_{ik}.$$

When the procedure is complete, the effects of the off-nominal turns ratios are included directly in $\widetilde{Y}$. For notational convenience, this correction procedure is written with respect to an already constructed admittance matrix $\widetilde{Y}$. In practice, the corrections are made in the initial construction of $\widetilde{Y}$, as given in §4.1.4, rather than performed as a replacement procedure.

REMARK 4.2. A transformer with off-nominal magnitude only (real valued a) leaves $\widetilde{Y}$ a symmetric matrix, but a phase-shifting transformer (complex a) does not.

4.1.4. Construction Equations for Admittance Matrix. In general, any of the branch elements described above can be represented by a series admittance $\widetilde{y}_{ik}$, a shunt admittance $\widetilde{y}_{ik}^{\text{Sh}}$, and a complex turns ratio (nominal or off-nominal) $a_{ik} = T_{ik}e^{j\varphi_{ik}}$. Using (4.4) and the correction procedure given in §4.1.3, the entries of $\widetilde{Y}$ become

$$\widetilde{Y}_{ii} = \widetilde{y}_i^{\text{S}} + \sum_{k:(i,k)\in\mathbf{L}} \frac{1}{|a_{ik}|^2}\left(\widetilde{y}_{ik} + \frac{1}{2}\widetilde{y}_{ik}^{\text{Sh}}\right) + \sum_{k:(k,i)\in\mathbf{L}} \left(\widetilde{y}_{ki} + \frac{1}{2}\widetilde{y}_{ki}^{\text{Sh}}\right), \tag{4.9}$$

$$\widetilde{Y}_{ik} = -\sum_{k:(i,k)\in\mathbf{L}} \frac{1}{a_{ik}^*}\widetilde{y}_{ik} - \sum_{k:(k,i)\in\mathbf{L}} \frac{1}{a_{ik}}\widetilde{y}_{ki}, \quad i \neq k \tag{4.10}$$

TABLE 4.1

Branch impedance data for Example 4.3. All quantities except phase angles are given in per-unit. Dots indicate nominal voltage ratios and phase angles.

From Bus i	To Bus k	Series Resistance R_{ik}	Series Reactance X_{ik}	Shunt Susceptance b^{Sh}_{ik}	Voltage Ratio T_{ik}	Phase Angle φ_{ik}
1	2	0.000	0.300	0.000	·	·
1	3	0.023	0.145	0.040	·	·
2	4	0.006	0.032	0.010	·	·
3	4	0.020	0.260	0.000	·	$-3.0°$
3	5	0.000	0.320	0.000	0.98	·
4	5	0.000	0.500	0.000	·	·

where $a = 1$ for any branch with a nominal turns ratio. Equations (4.9)–(4.10) can also be separated until real and imaginary parts using the definition $\widetilde{Y} = G + jB$ and the identity $a_{ik} = T_{ik}\left(\cos\varphi_{ik} + j\sin\varphi_{ik}\right)$,

$$G_{ii} = g_i^{\mathrm{S}} + \sum_{k:(i,k)\in\mathbf{L}} \frac{1}{T_{ik}^2}\left(g_{ik} + \frac{1}{2}g_{ik}^{\mathrm{Sh}}\right) + \sum_{k:(k,i)\in\mathbf{L}}\left(g_{ki} + \frac{1}{2}g_{ki}^{\mathrm{Sh}}\right), \tag{4.11}$$

$$\begin{aligned} G_{ik} = &-\sum_{k:(i,k)\in\mathbf{L}} \frac{1}{T_{ik}}\left(g_{ik}\cos\varphi_{ik} - b_{ik}\sin\varphi_{ik}\right) \\ &- \sum_{k:(k,i)\in\mathbf{L}} \frac{1}{T_{ki}}\left(g_{ki}\cos\varphi_{ki} + b_{ki}\sin\varphi_{ki}\right), \quad i \neq k \end{aligned} \tag{4.12}$$

$$B_{ii} = b_i^{\mathrm{S}} + \sum_{k:(i,k)\in\mathbf{L}} \frac{1}{T_{ik}^2}\left(b_{ik} + \frac{1}{2}b_{ik}^{\mathrm{Sh}}\right) + \sum_{k:(k,i)\in\mathbf{L}}\left(b_{ki} + \frac{1}{2}b_{ki}^{\mathrm{Sh}}\right), \tag{4.13}$$

$$\begin{aligned} B_{ik} = &-\sum_{k:(i,k)\in\mathbf{L}} \frac{1}{T_{ik}}\left(g_{ik}\sin\varphi_{ik} + b_{ik}\cos\varphi_{ik}\right) \\ &- \sum_{k:(k,i)\in\mathbf{L}} \frac{1}{T_{ki}}\left(-g_{ki}\sin\varphi_{ki} + b_{ki}\cos\varphi_{ki}\right) \quad i \neq k. \end{aligned} \tag{4.14}$$

EXAMPLE 4.3. *Table 4.1 provides a set of branch data for the 5-bus example system of Figure 3.1. Note that branch* $(3,4)$ *is a phase-shifting transformer and branch* $(4,5)$ *has an off-nominal voltage ratio. In addition to the branch data, bus 2 has a shunt susceptance of* $j0.30$ *pu and bus 3 has a shunt conductance of* 0.05 *pu.*

To compute the admittance matrix for this system, we first compute the series admittance $\widetilde{y}_{ik}$ *of each branch using* (4.5). *For example, the series admittance of branch* $(1,3)$ *is*

$$\widetilde{y}_{13} = \frac{0.023}{0.023^2 + 0.145^2} - j\frac{0.145}{0.023^2 + 0.145^2} \approx 1.067 - j6.727.$$

The remaining branches have series admittances

$$\begin{aligned} \widetilde{y}_{12} &\approx 0.000 - j3.333, \\ \widetilde{y}_{24} &\approx 5.660 - j30.189, \\ \widetilde{y}_{34} &\approx 0.294 - j3.824, \\ \widetilde{y}_{35} &\approx 0.000 - j3.125, \end{aligned}$$

and

$$\widetilde{y}_{45} \approx 0.000 - j2.000.$$

Verification of these values is left as an exercise for the reader.

Next, we construct $\widetilde{Y}$ *using* (4.9)–(4.10). *For example, diagonal element* $\widetilde{Y}_{33}$ *consists of summing the admittances of branches* $(1,3)$, $(3,4)$, *and* $(3,5)$, *plus the contributions of the shunt conductance at bus 3 and the shunt susceptance of branch* $(1,3)$. $\widetilde{y}_{34}$ *and* $\widetilde{y}_{35}$ *have off-nominal turns ratios*

$$a_{34} = 1.0e^{-j3.0^\circ} \approx 0.999 - j0.052$$

and

$$a_{35} = 0.98e^{-j0.0^\circ} = 0.980.$$

(Note that $a_{34}a_{34}^* = 1.0$ *if rounding errors are neglected.) Therefore, the full expression for* $\widetilde{Y}_{33}$ *is*

$$\begin{aligned}
\widetilde{Y}_{33} &\approx (1.067 - j6.727) + j\frac{0.04}{2} + \frac{0.294 - j3.824}{(0.999 - j0.052)\,(0.999 + j0.052)} - \frac{j3.125}{0.980^2} + 0.05, \\
&\approx 1.41 - j13.78.
\end{aligned}$$

An example off-diagonal element is $\widetilde{Y}_{34}$, *which from* (4.10) *is*

$$\widetilde{Y}_{34} \approx -\frac{0.294 - j3.824}{(0.999 + j0.052)} \approx -0.09 + j3.83.$$

The full admittance matrix is

$$\widetilde{Y} \approx \begin{pmatrix} 1.07 - j10.04 & 0.00 + j3.33 & -1.07 + j6.73 & 0 & 0 \\ 0.00 + j3.33 & 5.66 - j33.22 & 0 & -5.66 + j30.19 & 0 \\ -1.07 + j6.73 & 0 & 1.41 - j13.78 & -0.09 + j3.83 & 0.00 + j3.19 \\ 0 & -5.66 + j30.19 & -0.49 + j3.80 & 5.95 - j36.01 & 0.00 + j2.00 \\ 0 & 0 & 0.00 + j3.19 & 0.00 + j2.00 & 0.00 - j5.13 \end{pmatrix}.$$

Verification of the remaining matrix elements is left as an exercise for the reader. □

4.2. AC Power Flow. For a given $\widetilde{Y}$, equation (4.2) can be decomposed into a set of equations for the real and reactive power injections by evaluating the real and imaginary parts of S, respectively. This process yields a pair of equations called the AC power flow equations, which can be written in several equivalent forms depending on whether the voltages and admittance matrix elements are expressed in polar or rectangular coordinates. In the literature, the most common forms of the AC power flow equations are (in order)

1. Selection of polar coordinates for voltage, $\widetilde{V}_i = V_i\angle\delta_i$, and rectangular coordinates for admittance, $\widetilde{Y}_{ik} = G_{ik} + jB_{ik}$:

$$P_i\left(V,\delta\right) = V_i\sum_{k=1}^{N} V_k\big(G_{ik}\cos\left(\delta_i - \delta_k\right) + B_{ik}\sin\left(\delta_i - \delta_k\right)\big) \tag{4.15}$$

$$Q_i\left(V,\delta\right) = V_i\sum_{k=1}^{N} V_k\big(G_{ik}\sin\left(\delta_i - \delta_k\right) - B_{ik}\cos\left(\delta_i - \delta_k\right)\big) \tag{4.16}$$

2. Selection of polar coordinates for voltage, $\widetilde{V}_i = V_i \angle \delta_i$, and polar coordinates for admittance, $\widetilde{Y}_{ik} = Y_{ik} \angle \theta_{ik}$:

$$P_i\left(V, \delta\right) = V_i \sum_{k=1}^{N} V_k Y_{ik} \cos\left(\delta_i - \delta_k - \theta_{ik}\right) \tag{4.17}$$

$$Q_i\left(V, \delta\right) = V_i \sum_{k=1}^{N} V_k Y_{ik} \sin\left(\delta_i - \delta_k - \theta_{ik}\right) \tag{4.18}$$

3. Selection of rectangular coordinates for voltage, $\widetilde{V}_i = E_i + jF_i$, and rectangular coordinates for admittance, $\widetilde{Y}_{ik} = G_{ik} + jB_{ik}$:

$$P_i\left(E, F\right) = \sum_{k=1}^{N} G_{ik}\left(E_i E_k + F_i F_k\right) + B_{ik}\left(F_i E_k - E_i F_k\right) \tag{4.19}$$

$$Q_i\left(E, F\right) = \sum_{k=1}^{N} G_{ik}\left(F_i E_k - E_i F_k\right) - B_{ik}\left(E_i E_k + F_i F_k\right) \tag{4.20}$$

Power systems texts [14, 32, 37] provide exact derivations of these three forms of the AC power flow equations.[3] Each form of the equations involves real-valued quantities only. However, all forms are equivalent and give the exact solution to the power flow under the assumptions outlined in §3.1.

From an OPF perspective, there is little difference between the selection of polar or rectangular coordinates for the admittance matrix. Rectangular coordinates are more common in practice because they facilitate the use of certain approximations in fast-decoupled solution methods for conventional PF [37]. These approximations are also useful in the development of the DC power flow equations; see §4.3. Rectangular coordinates also facilitate the inclusion of transformer voltage ratios and phase angles as decision variables. However, neither of these advantages strongly affects the AC power flow equations as used in most OPF formulations.

The more important distinction is the choice of polar or rectangular coordinates for voltage. The advantage of voltage polar coordinates is that constraints on the voltage magnitude can be enforced directly,

$$\begin{aligned} V_i &\geq V_i^{\min}, \\ V_i &\leq V_i^{\max}. \end{aligned}$$

In voltage rectangular coordinates, on the other hand, voltage magnitude limits require the functional inequality constraints

$$\begin{aligned} \sqrt{E_i^2 + F_i^2} &\geq V_i^{\min}, \\ \sqrt{E_i^2 + F_i^2} &\leq V_i^{\max}. \end{aligned}$$

Similarly, if the voltage magnitude is fixed (for instance at a PV bus; see §4.4), then in polar coordinates V_i can be replaced with a constant value. In rectangular coordinates, however, a fixed voltage magnitude requires the equality constraint

$$\sqrt{E_i^2 + F_i^2} = V_i.$$

[3] A fourth form—selection of rectangular coordinates for voltage and polar coordinates for admittance—is theoretically possible but has no advantages for practical use.

TABLE 4.2

Comparison of the selection of voltage polar coordinates versus voltage rectangular coordinates for the power flow equations. Bold entries indicate the superior characteristic.

	Polar Coords.	Rectangular Coords.
Voltage magnitude limit	**Variable limit**	Nonlinear functional inequality constraint
Fixed voltage magnitude	**Variable elimination by substitution**	Nonlinear functional equality constraint
# of variables in conventional PF	$\boldsymbol{N+M-1}$	$2N-2$
Nature of PF equations	Trigonometric	**Quadratic**
1^{st} derivative of PF equations	Trigonometric	**Linear**
2^{nd} derivative of PF equations	Trigonometric	**Constant**

Thus, for a fixed voltage magnitude, use of voltage polar coordinates leads to a reduction of variables while use of voltage rectangular coordinates leads to an increase in (non-linear, non-convex) equality constraints. For this reason, polar coordinates are preferred both for conventional PF and most OPF formulations.

There is, however, one compelling reason to use voltage rectangular coordinates: expressing voltage in rectangular coordinates eliminates trigonometric functions from the power flow equations. The resulting power flow equations (4.19)–(4.20) are quadratic, which presents several advantages [30]:

1. The elimination of trigonometric functions speeds evaluation of the equations.
2. The 2^{nd} order Taylor series expansion of a quadratic function is exact; this yields an efficiency advantage in higher-order interior-point algorithms for OPF.
3. The Hessian matrix for a quadratic function is constant and need be evaluated only once. This simplifies the application of Newton's method to the KKT conditions of the OPF formulation.

In some cases, these computational advantages outweigh the disadvantages associated with enforcing voltage magnitude constraints. Table 4.2 summarizes the differences between the two voltage coordinate choices.

EXAMPLE 4.4. *Using the admittance matrix developed in Example 4.3, we can write the real and reactive power flow equations for any bus in the 5-bus example system. From* (4.15)*, the real power injection at bus 1 is*

$$\begin{aligned}
P_1(V,\delta) &= V_1 \sum_{k=1}^{5} V_k\big(G_{1k}\cos(\delta_1-\delta_k) + B_{1k}\sin(\delta_1-\delta_k)\big),\\
&\approx 1.07V_1^2\cos(\delta_1-\delta_1) - 1.07V_1V_3\cos(\delta_1-\delta_3) - 10.04V_1^2\sin(\delta_1-\delta_1)\\
&\quad + 3.33V_1V_2\sin(\delta_1-\delta_2) + 6.73V_1V_3\sin(\delta_1-\delta_3),\\
&\approx 1.07V_1^2 - 1.07V_1V_3\cos(\delta_1-\delta_3) + 3.33V_1V_2\sin(\delta_1-\delta_2)\\
&\quad + 6.73V_1V_3\sin(\delta_1-\delta_3).
\end{aligned}$$

Similarly, from (4.16)*, the reactive power injection at bus 1 is*

$$\begin{aligned}
Q_1(V,\delta) &= V_1 \sum_{k=1}^{5} V_k \big(G_{1k} \sin(\delta_1 - \delta_k) - B_{1k} \cos(\delta_1 - \delta_k) \big), \\
&\approx 1.07 V_1^2 \sin(\delta_1 - \delta_1) - 1.07 V_1 V_3 \sin(\delta_1 - \delta_3) + 10.04 V_1^2 \cos(\delta_1 - \delta_1) \\
&\quad - 3.33 V_1 V_2 \cos(\delta_1 - \delta_2) - 6.73 V_1 V_3 \cos(\delta_1 - \delta_3), \\
&\approx -1.07 V_1 V_3 \sin(\delta_1 - \delta_3) + 10.04 V_1^2 - 3.33 V_1 V_2 \cos(\delta_1 - \delta_2) \\
&\quad - 6.73 V_1 V_3 \cos(\delta_1 - \delta_3).
\end{aligned}$$

Evaluation of the remaining buses is left as an excercise for the reader. □

4.3. DC Power Flow. The AC power flow equations are nonlinear. For conventional PF, this nonlinearity requires the use of an iterative numerical method; for OPF it implies both a nonlinear formulation and non-convexity in the feasible region. In order to simplify the system representation, power systems engineers have developed a linear approximation to the power flow equations. This approximation is called DC power flow.[4]

The conventional development of the DC power flow equations requires several assumptions regarding the power system [26,37]:

1. All system branch resistances are approximately zero, that is, the transmission system is assumed to be lossless. As a result, all $\theta_{ik} = \pm 90°$ and all $G_{ik} = 0$.
2. The differences between adjacent bus voltage angles are small, such that $\sin(\delta_i - \delta_k) \approx \delta_i - \delta_k$ and $\cos(\delta_i - \delta_k) \approx 1$.
3. The system bus voltages are approximately equal to 1.0. This assumption requires that there is sufficient reactive power generation in the system to maintain a level voltage profile.
4. Reactive power flow is neglected.

Applying these assumptions to (4.15) produces the DC power flow equation

$$P_i(\delta) \approx \sum_{k=1}^{N} B_{ik} (\delta_i - \delta_k) \tag{4.21}$$

Under normal system operating conditions, DC power flow models real power transfer quite accurately. It has been successfully used in many OPF applications that require rapid and robust solutions. However, the assumptions required for DC power flow can lead to significant errors for stressed systems. The exact equation for branch power transfer is

$$P_{ik} = g_{ik} V_i^2 - g_{ik} V_i V_k \cos(\delta_i - \delta_k) - b_{ik} V_i V_k \sin(\delta_i - \delta_k), \tag{4.22}$$

cf. (4.15), while the DC power flow approximation is

$$P_{ik} \approx -b_{ik} \sin(\delta_i - \delta_k). \tag{4.23}$$

The b_{ik} term dominates the exact expression because $V_i^2 \approx V_i V_k \cos(\delta_i - \delta_k)$ and therefore the first two terms in (4.22) largely cancel.

We observe that (4.23) overestimates the magnitude of the branch power transfer (4.22) if

[4]The DC power flow is so named because the equations resemble the power flow in a direct current (DC) network. However, the DC power flow equations still model an AC power system.

(i) The bus voltages at either end of the branch are depressed relative to the assumed value of 1.0 p.u., or

(ii) The angle difference between the buses is too large.

Observation (ii) follows from the relationship $|\sin(\delta_i - \delta_k)| \leq |\delta_i - \delta_k|$. Depressed voltages and larger than normal angle differences are common in stressed power systems. In particular, large differences in voltage in different areas of the system can lead to significant error [28]. Therefore, the DC power flow equations should not be used for OPF under stressed system conditions unless they have been carefully evaluated for accuracy in the system under test.

EXAMPLE 4.5. *Consider a transmission line from bus i to bus k with admittance* $0.05 - j2.0$. *Let* $\widetilde{V}_i = 0.95 \angle 0^\circ$ *and* $\widetilde{V}_k = 0.90 \angle -20^\circ$. *(These numbers do not represent normal operation, but are plausible for a stressed power system. Operating voltages as low as 0.9 p.u. are allowable in emergency conditions, and angle differences of up to ±30° can occur on long, heavily loaded transmission lines.)*

The exact power transfer for this line is

$$\begin{aligned} P_{ik} &= 0.05 \cdot 0.95^2 - 0.05 \cdot 0.95 \cdot 0.90 \cos(0^\circ + 20^\circ) - 2.0 \cdot 0.95 \cdot 0.90 \sin(0^\circ + 20^\circ), \\ &= 0.590 \ p.u. \end{aligned}$$

The approximate power transfer is

$$\begin{aligned} P_{ik} &\approx -2.0 \sin(0^\circ + 20^\circ), \\ &\approx 0.684 \ p.u. \end{aligned}$$

The error in the approximate power transfer is 16%; most of this error is attributable to the voltage difference. □

Even under normal operation, the approximation of a lossless transmission network can also lead to significant errors in generator scheduling, branch power flow estimates, and marginal fuel cost estimates. Power transfer errors for certain critically loaded branches can be much higher than the average branch error. Therefore, in practical DC power flow models an estimate of the losses must be reintroduced using approximate methods, especially if the network is large [28].

For further discussion regarding the advantages and disadvantages of DC power flow, including loss approximation methods, we refer the interested reader to [25, 28]. Throughout the rest of this primer, we use the AC power flow equations.

4.4. Solution Methods for Conventional PF. Many practical OPF algorithms incorporate aspects of conventional PF solution methods. Therefore, a basic understanding of these methods is helpful when reviewing OPF literature. Here, we discuss the solution of the AC power flow equations with voltage polar coordinates. The solution method for voltage rectangular coordinates is similar; Zhu [37] provides a good summary.

Each system bus has four variables (real power injection P_i, reactive power injection Q_i, voltage magnitude V_i, and voltage angle δ_i) and is governed by two equations: either (4.15)–(4.16) or (4.17)–(4.18). Thus, a unique solution to the conventional PF requires fixing the values of two out of four variables at each bus.

REMARK 4.6. Even though the power flow equations are nonlinear, there exists only one physically meaningful solution for most power systems models given an equal number of equations and unknowns. Other solutions may exist mathematically, but have no realistic physical interpretation. (An example would be any solution which returns a negative voltage magnitude, as magnitudes are by definition nonnegative.)

Table 4.3
Power system bus types and characteristics for conventional power flow.

Bus Type	Slack	PQ	PV
# of buses in system	1	M	$N-M-1$
Known quantities	δ, V	P, Q	P, V
Unknown quantities	P, Q	δ, V	δ, Q
# of equations in conventional PF	0	2	1

In conventional PF, all system buses are assigned to one of three bus types:

Slack Bus At the slack bus, the voltage magnitude and angle are fixed and the power injections are free. There is only one slack bus in a power system.

Load Bus At a load bus, or PQ bus, the power injections are fixed while the voltage magnitude and angle are free. There are M PQ buses in the system.

Voltage-Controlled Bus At a voltage controlled bus, or PV bus, the real power injection and voltage magnitude are fixed while the reactive power injection and the voltage angle are free. (This corresponds to allowing a local source of reactive power to regulate the voltage to a desired setpoint.) There are $N-M-1$ PV buses in the system.

Assigning buses in this way establishes an equal number of equations and unknowns. Table 4.3 summarizes the three bus types.

If all voltage magnitudes and angles in the system are known, then the power injections are fully determined. Solving the power flow therefore requires determining $N-1$ voltage angles (corresponding to the PQ and PV buses) and M voltage magnitudes (corresponding to the PQ buses only). This is done by solving $N+M-1$ simultaneous nonlinear equations with known right hand side values. This equation set consists of the real power injection equation (4.15) at each PV and PQ bus and the reactive power injection equation (4.16) at each PQ bus.

Newton's method is commonly used to solve this system. The 1[st] order Taylor series approximation about the current estimate of V and δ yields

$$\begin{aligned}\begin{pmatrix}\Delta P \\ \Delta Q\end{pmatrix} &\approx \begin{pmatrix}\dfrac{\partial P}{\partial \delta} & \dfrac{\partial P}{\partial V} \\ \dfrac{\partial Q}{\partial \delta} & \dfrac{\partial Q}{\partial V}\end{pmatrix}\begin{pmatrix}\Delta \delta \\ \Delta V\end{pmatrix}, \\ &\approx J\begin{pmatrix}\Delta \delta \\ \Delta V\end{pmatrix}, \end{aligned} \tag{4.24}$$

where J is the Jacobian matrix of the system. At each iteration, the mismatches in the power flow equations are

$$\Delta P_i = \left(P_i^{\mathrm{G}} - P_i^{\mathrm{L}}\right) - P_i\left(V, \delta\right), \tag{4.25}$$

$$\Delta Q_i = \left(Q_i^{\mathrm{G}} - Q_i^{\mathrm{L}}\right) - Q_i\left(V, \delta\right). \tag{4.26}$$

Newton's method consists of iteratively solving (4.24) for the $\Delta\delta$ and ΔV required to correct the mismatch in the power flow equations computed from (4.25)–(4.26). Newton's method is locally quadratically convergent. Therefore, given a sufficiently good starting point, the method reliably finds the correct solution to the PF equations. Newton's method for conventional PF is described more fully in power systems texts [14, 32, 37].

In OPF, the decision variables are often partitioned into a set of control (independent) variables u and a set of state (dependent) variables x [7,10]. At each search step, the OPF algorithm fixes u and derives x by solving a conventional PF. When this method is used, the Jacobian matrix J plays several important roles:

1. It provides the linearization of the power flow equations required for successive linear programming (SLP) OPF algorithms,
2. It provides sensitivities in the power flow injections with respect to the state variables,
3. It provides a direct calculation of portions of the Hessian matrix of the Lagrangian function in OPF (see [29]), and
4. It is therefore often used to improve computational efficiency in computing the KKT conditions for the Lagrangian function.

In DC power flow, there is no distinction between PV and PQ buses because all voltage magnitudes are considered to be 1.0. As with the AC power flow, the slack bus angle is fixed. Because the DC power flow equations are linear, they may be solved directly for the voltage angles using

$$\delta = B^{-1}P.$$

(This is simply a solved matrix representation of (4.21).)

4.5. Practical Considerations. In our experience, there are several practical and computational aspects of OPF stemming from the power flow equations that can cause confusion. One of these is the use of the per-unit system, which is discussed in §3.4. We discuss a few others here.

4.5.1. Degrees versus Radians. Power systems engineers usually report angles in degrees, including in data files for OPF (see §6). For computation, these angles must be converted to radians, for two reasons:

1. Nearly all optimization software and descriptive languages—including AMPL and GAMS—implement trigonometric functions in radians, not degrees.
2. Even when using the DC power flow equations (which require no trigonometric function evaluations), radians must be used. If degrees are used, the powers computed from DC power flow will have a scaling error of $180/\pi$.

Power flow software typically handles these conversions transparently, accepting input and giving output in degrees. Thus, it can be difficult to remember that general-purpose optimization software requires an explicit conversion.

4.5.2. System Initialization. In both conventional power flow and OPF, the convergence of the power flow equations depends strongly on the selection of a starting point. Given a starting point far from the correct solution, the power flow equations may converge to a meaningless solution, or may not converge at all. In the absence of a starting point, standard practice is to initialize all voltage magnitudes to 1.0 p.u. and all voltage angles to zero; this is called a “cold start” or a “flat start”.

The alternative is a “hot start”, in which the voltages and angles are initialized to the solution of a pre-solved power flow. Hot starts are often used in online OPF to minimize computation time and ensure that the search begins from the current system operating condition.

4.5.3. Decoupled Power Flow versus Decoupled OPF. In practical power systems, real power injections are strongly coupled to voltage angles and reactive power injections are strongly coupled to voltage magnitudes. Conversely, real power injections are weakly coupled to voltage magnitudes and reactive power injections are weakly coupled to voltage angles. This feature has led to the development of decoupled solution methods for the power flow equations [14, 37]. The most basic decoupling method is to use a set of approximate Taylor series expansions of the form

$$\Delta P \approx \frac{\partial P}{\partial \delta} \Delta \delta,$$
$$\Delta Q \approx \frac{\partial Q}{\partial V} \Delta V.$$

This allows the use of separate Newton updates for δ and V with correspondingly smaller matrices; this is a significant computational advantage.

Although decoupled power flow uses an approximate update method, it still uses exact real and reactive power mismatches ΔP and ΔQ from (4.25)–(4.26) and updates both V and δ at each iteration. Decoupled power flow therefore is locally convergent to the exact solution to the power flow. However, because of the approximated Jacobian matrix, more iterations are required for convergence [14]. Zhu [37] discusses several decoupled power flow variants in detail.

Decoupled OPF also takes advantage of the strong P-δ and Q-V relationships by formulating a real subproblem and a reactive subproblem. The optima of the subproblems are assumed to be independent. Unlike decoupled power flow, however, decoupled OPF solves the subproblems sequentially rather than simultaneously: the real subproblem solves for the optimal values of P and δ while holding Q and V constant, and the reactive subproblem solves for the optimal values of Q and V while holding P and δ constant [9, 29]. Decoupled OPF is therefore distinctly different from decoupled power flow in that the decoupled OPF solution is inexact. The error is a function of the accuracy of the decoupling assumptions; these assumptions should therefore be evaluated for accuracy if a decoupled OPF approach is considered.

REMARK 4.7. In the OPF literature, it is not always clear whether decoupled OPF is in use or whether a decoupled power flow procedure is used within the solution algorithm for a coupled OPF. Because of the implications for the OPF solution quality, the careful reader should try to discern which is the case.

5. Optimal Power Flow.

Broadly speaking, any power systems optimization problem which includes the power flow equations in the set of equality constraints is an OPF problem. Thus, the term OPF now encompasses an extremely wide variety of formulations, many with tailored solution methods [11]. Most of these variants, however, build upon the classic formulation of Carpentier [8] and Dommel and Tinney [10]. (This is so common that most OPF papers omit the core of the formulation entirely, focusing only on novel enhancements or algorithmic development.) Here, we first present the classical formulation and then briefly discuss several common extensions.

5.1. Classical Formulation.

The classical OPF formulation of Dommel and Tinney is an extension of economic dispatch (ED): its objective is to minimize the total cost of electricity generation while maintaining the electric power system within safe operating limits. The power system is modeled as a set of buses $\mathbf{N}$ connected by a set of branches $\mathbf{L}$. Controllable generators are located at a subset $\mathbf{G}$ of the system buses. The operating cost of each generator is a (typically quadratic) function of its real output power: $C_i\left(P_i^{\mathrm{G}}\right)$. The objective is to minimize the total cost of generation.

The classical form of the formulation is

$$\begin{aligned}
\min \quad & \sum_{i \in \mathbf{G}} C_i\left(P_i^{\mathrm{G}}\right), && && (5.1)\\
\text{s.t.} \quad & P_i\left(V, \delta\right) = P_i^{\mathrm{G}} - P_i^{\mathrm{L}} && \forall\, i \in \mathbf{N}, && (5.2)\\
& Q_i\left(V, \delta\right) = Q_i^{\mathrm{G}} - Q_i^{\mathrm{L}} && \forall\, i \in \mathbf{N}, && (5.3)\\
& P_i^{\mathrm{G,min}} \le P_i^{\mathrm{G}} \le P_i^{\mathrm{G,max}} && \forall\, i \in \mathbf{G}, && (5.4)\\
& Q_i^{\mathrm{G,min}} \le Q_i^{\mathrm{G}} \le Q_i^{\mathrm{G,max}} && \forall\, i \in \mathbf{G}, && (5.5)\\
& V_i^{\min} \le V_i \le V_i^{\max} && \forall\, i \in \mathbf{N}, && (5.6)\\
& \delta_i^{\min} \le \delta_i \le \delta_i^{\max} && \forall\, i \in \mathbf{N}. && (5.7)
\end{aligned}$$

In (5.2)–(5.3), $P_i\left(V, \delta\right)$ and $Q_i\left(V, \delta\right)$ represent the power flow equations in polar form—either (4.15)–(4.16) or (4.17)–(4.18). The vector of control variables (independent decision variables) is

$$u = \left(P_{i:i \in \mathbf{G}}^{\mathrm{G}}, Q_{i:i \in \mathbf{G}}^{\mathrm{G}}\right)$$

and the vector of state variables (dependent decision variables) is

$$x = \left(\delta_2, \ldots, \delta_N, V_2, \ldots, V_N\right).$$

The voltage magnitude and angle at the system slack bus (by convention, bus 1) are fixed, usually to $\widetilde{V}_1 = 1.0\angle 0$.

If the system contains controllable phase-shifting or tap-changing transformers, then the corresponding phase angles and tap ratios are introduced into the set of control variables. The control variable vector u becomes

$$u = \left(P_{i:i \in \mathbf{G}}^{\mathrm{G}}, Q_{i:i \in \mathbf{G}}^{\mathrm{G}}, \varphi_{ik:ik \in \mathbf{H}}, T_{ik:ik \in \mathbf{K}}\right),$$

where $\mathbf{H}$ and $\mathbf{K}$ are the sets of branches with controllable-phase shifting transformers and tap-changing transformers, respectively. Since φ and T alter the elements of admittance matrix $\widetilde{Y}$, the left hand sides of (5.2) and (5.3) become functions of φ and T: $P_i\left(V, \delta, \varphi, T\right)$ and $Q_i\left(V, \delta, \varphi, T\right)$, respectively. The formulation is also augmented with bound constraints on the phase angles

$$\varphi_{ik}^{\min} \le \varphi_{ik} \le \varphi_{ik}^{\max} \qquad \forall\, ik \in \mathbf{H} \tag{5.8}$$

and the tap ratios

$$T_{ik}^{\min} \le T_{ik} \le T_{ik}^{\max} \qquad \forall\, ik \in \mathbf{K}. \tag{5.9}$$

Although not considered in the earliest papers, more recent OPF formulations also consider branch current limits. Unlike the previous bounds, the branch current limits require functional inequality constraints. By Ohm's law, the current magnitude in branch ik is

$$I_{ik} = \left|\widetilde{V}_i - \widetilde{V}_k\right| y_{ik}, \tag{5.10}$$

TABLE 5.1
Bus data for Example 5.2. All quantities are given in per-unit. Dots indicates zero values.

Bus i	Load Real Power P_i^{L}	Load Reactive Power Q_i^{L}	Min. Bus Voltage $V_i^{\min}$	Max. Bus Voltage $V_i^{\max}$
1	·	·	1.00	1.00
2	·	·	0.95	1.05
3	·	·	0.95	1.05
4	0.900	0.400	0.95	1.05
5	0.239	0.129	0.95	1.05

TABLE 5.2
Generator data for Example 5.2. All quantities are given in per-unit.

Bus i	Min. Generator Real Power $P_i^{\mathrm{G,min}}$	Max. Generator Real Power $P_i^{\mathrm{G,max}}$	Min. Generator Reactive Power $Q_i^{\mathrm{G,min}}$	Max. Generator Reactive Power $Q_i^{\mathrm{G,max}}$
1	$-\infty$	∞	$-\infty$	∞
3	0.10	0.40	-0.20	0.30
4	0.05	0.40	-0.20	0.20

where y_{ik} is the magnitude of the branch admittance. Thus, we can constrain the branch current using

$$\begin{aligned} \left|\widetilde{V}_i - \widetilde{V}_k\right| y_{ik} &\le I_{ik}^{\max}, \\ \Leftrightarrow \quad \sqrt{\left(V_i \cos\delta_i - V_k \cos\delta_k\right)^2 + \left(V_i \sin\delta_i - V_k \sin\delta_k\right)^2} &\le \frac{I_{ik}^{\max}}{y_{ik}}, \\ \Leftrightarrow \quad \left(V_i \cos\delta_i - V_k \cos\delta_k\right)^2 + \left(V_i \sin\delta_i - V_k \sin\delta_k\right)^2 &\le \frac{\left(I_{ik}^{\max}\right)^2}{y_{ik}^2} \quad \forall\, ik \in \mathbf{L}. \end{aligned} \tag{5.11}$$

Rather than bounding the square of the current as is given in (5.11), many formulations bound the total real and reactive power flow entering the line. However, (5.11) gives a more exact representation of the true constraint, which is technically a maximum current, not a maximum power.

REMARK 5.1. For branches with off-nominal turns ratios, the tap bus voltage V_i and angle δ_i in (5.11) must be corrected for the off-nominal turns ratio. In this case, V_i is replaced by $V_i' = V_i/T_{ik}$ and δ_i is replaced by $\delta_i' = \delta_i - \varphi_{ik}$.

Even without variable phase angles, variable tap ratios, or branch current limits, the classical OPF formulation is difficult to solve. The power flow constraints (5.2)–(5.3) are both nonlinear and non-convex, and the presence of trigonometric functions complicates the construction of approximations. For this reason, OPF problems have historically been solved using tailored algorithms rather than general purpose solvers.

EXAMPLE 5.2. *We now develop the classical OPF formulation for the 5-bus example system first presented in Figure 3.1. For this example, the branch impedance data are as given in Table 4.1, except that we assign φ_{34} and T_{35} to be decision variables representing a phase shifting transformer and an on-load tap changer, respectively. φ_{34} and T_{35} have limits*

$$-30.0^\circ \le \varphi_{34} \le 30.0^\circ$$

and

$$0.95 \leq T_{35} \leq 1.05.$$

Consider the bus data (voltage limits, load, and generation) given in Tables 5.1 and 5.2. The system power base is 100 MW. Given this data, the sets defining the formulation are:

$$\begin{aligned}
\mathbf{N} &= \{1, 2, 3, 4, 5\}, \\
\mathbf{G} &= \{1, 3, 4\}, \\
\mathbf{L} &= \{(1,2), (1,3), (2,4), (3,4), (3,5), (4,5)\}, \\
\mathbf{H} &= \{(3,4)\},
\end{aligned}$$

and

$$\mathbf{K} = \{(3,5)\}.$$

The three generator cost functions, in thousands of dollars, are

$$\begin{aligned}
C_1\left(P_1^{\mathrm{G}}\right) &= 0.35 P_1^{\mathrm{G}}, \\
C_3\left(P_3^{\mathrm{G}}\right) &= 0.20 P_3^{\mathrm{G}} + 0.40\left(P_3^{\mathrm{G}}\right)^2, \\
C_4\left(P_4^{\mathrm{G}}\right) &= 0.30 P_4^{\mathrm{G}} + 0.50\left(P_4^{\mathrm{G}}\right)^2,
\end{aligned}$$

where the P_i^{G} are expressed in per-unit.

To develop the full formulation, it is first necessary to re-write $\widetilde{Y}$ from Example 4.3 to explicitly include φ_{34} and T_{35}. Let

$$a_{34} = \cos\varphi_{34} + j\sin\varphi_{34}$$

and

$$a_{35} = T_{35}.$$

(Note that $a_{34}a_{34}^* = 1.0$, $1/a_{34} = \cos\varphi_{34} - j\sin\varphi_{34} = a_{34}^*$, and $1/a_{34}^* = \cos\varphi_{34} + j\sin\varphi_{34} = a_{34}$.) Then, using (4.9)–(4.10) and simplifying,

$$\begin{aligned}
\widetilde{Y}_{33} &= 1.41 - j10.53 - j\frac{1}{T_{35}^2} \cdot 3.13, \\
\widetilde{Y}_{34} &= -0.29\cos\varphi_{34} - 3.82\sin\varphi_{34} + j\left(3.82\cos\varphi_{34} - 0.29\sin\varphi_{34}\right), \\
\widetilde{Y}_{43} &= -0.29\cos\varphi_{34} + 3.82\sin\varphi_{34} + j\left(3.82\cos\varphi_{34} + 0.29\sin\varphi_{34}\right), \\
\widetilde{Y}_{35} &= j\frac{1}{T_{35}} \cdot 3.13,
\end{aligned}$$

and

$$\widetilde{Y}_{53} = j\frac{1}{T_{35}} \cdot 3.13.$$

$\widetilde{Y}_{44}$, $\widetilde{Y}_{55}$, and the remaining matrix entries are unchanged.

Bus 1 is the system slack bus, and therefore $\widetilde{V}_1$ *is fixed to* $1.0\angle 0.0^{\circ}$*. To construct the formulation, we round all numerical values to two decimal places. (This rounding does not affect model feasibility because sufficient degrees of freedom exist in the state variables.) Following* (5.1)–(5.7), (5.8), *and* (5.9), *the full formulation is*

$$
\begin{aligned}
\min \quad & 0.35P_1^{\mathrm{G}} + 0.20P_3^{\mathrm{G}} + 0.40\left(P_3^{\mathrm{G}}\right)^2 + 0.30P_4^{\mathrm{G}} + 0.50\left(P_4^{\mathrm{G}}\right)^2, \\
\text{s.t.} \quad & P_1^{\mathrm{G}} = 1.07 - 1.07V_3\cos\left(-\delta_3\right) + 3.33V_2\sin\left(-\delta_2\right) + 6.73V_3\sin\left(-\delta_3\right), \\
& 0 = 5.66V_2^2 - 5.66V_2V_4\cos\left(\delta_2 - \delta_4\right) \\
& \qquad + 3.33V_2\sin\left(\delta_2\right) + 30.19V_2V_4\sin\left(\delta_2 - \delta_4\right), \\
& P_3^{\mathrm{G}} = 1.41V_3^2 - 1.07V_3\cos\left(\delta_3\right) \\
& \qquad + \left(-0.29\cos\varphi_{34} - 3.82\sin\varphi_{34}\right)V_3V_4\cos\left(\delta_3 - \delta_4\right) \\
& \qquad + 6.73V_3\sin\left(\delta_3\right) + \left(3.82\cos\varphi_{34} - 0.29\sin\varphi_{34}\right)V_3V_4\sin\left(\delta_3 - \delta_4\right) \\
& \qquad + \frac{3.13}{T_{35}}V_3V_5\sin\left(\delta_3 - \delta_5\right), \\
& P_4^{\mathrm{G}} - 0.900 = 5.95V_4^2 - 5.66V_4V_2\cos\left(\delta_4 - \delta_2\right) \\
& \qquad + \left(-0.29\cos\varphi_{34} + 3.82\sin\varphi_{34}\right)V_4V_3\cos\left(\delta_4 - \delta_3\right) \\
& \qquad + 30.19V_4V_2\sin\left(\delta_4 - \delta_2\right) \\
& \qquad + \left(3.82\cos\varphi_{34} + 0.29\sin\varphi_{34}\right)V_4V_3\sin\left(\delta_4 - \delta_3\right) + 2.00V_4V_5\sin\left(\delta_4 - \delta_5\right), \\
& -0.239 = \frac{3.13}{T_{35}}V_5V_3\sin\left(\delta_5 - \delta_3\right) + 2.00V_5V_4\sin\left(\delta_5 - \delta_4\right), \\
& Q_1^{\mathrm{G}} = 10.04 - 1.07V_3\sin\left(-\delta_3\right) - 3.33V_2\cos\left(-\delta_2\right) - 6.73V_3\cos\left(-\delta_3\right), \\
& 0 = -5.66V_2V_4\sin\left(\delta_2 - \delta_4\right) + 33.22V_2^2 \\
& \qquad - 3.33V_2\cos\left(\delta_2\right) - 30.19V_2V_4\cos\left(\delta_2 - \delta_4\right), \\
& Q_3^{\mathrm{G}} = -1.07V_3\sin\left(\delta_3\right) + \left(-0.29\cos\varphi_{34} - 3.82\sin\varphi_{34}\right)V_3V_4\sin\left(\delta_3 - \delta_4\right) \\
& \qquad + \left(10.53 + \frac{3.13}{T_{35}^2}\right)V_3^2 - 6.73V_3\cos\left(\delta_3\right) \\
& \qquad - \left(3.82\cos\varphi_{34} - 0.29\sin\varphi_{34}\right)V_3V_4\cos\left(\delta_3 - \delta_4\right) - \frac{3.13}{T_{35}}V_3V_5\cos\left(\delta_3 - \delta_5\right), \\
& Q_4^{\mathrm{G}} - 0.940 = -5.66V_4V_2\sin\left(\delta_4 - \delta_2\right) \\
& \qquad + \left(-0.29\cos\varphi_{34} + 3.82\sin\varphi_{34}\right)V_4V_3\sin\left(\delta_4 - \delta_3\right) \\
& \qquad + 36.01V_4^2 - 30.19V_4V_2\cos\left(\delta_4 - \delta_2\right) \\
& \qquad - \left(3.82\cos\varphi_{34} + 0.29\sin\varphi_{34}\right)V_4V_3\cos\left(\delta_4 - \delta_3\right) - 2.00V_4V_5\cos\left(\delta_4 - \delta_5\right), \\
& -0.129 = 5.13V_5^2 - \frac{3.13}{T_{35}}V_5V_3\cos\left(\delta_5 - \delta_3\right) - 2.00V_5V_4\cos\left(\delta_5 - \delta_4\right),
\end{aligned}
$$

$$\begin{aligned}
&0.10 \le P_3^{\mathrm{G}} \le 0.40,\\
&0.05 \le P_4^{\mathrm{G}} \le 0.40,\\
&-0.20 \le Q_3^{\mathrm{G}} \le 0.30,\\
&-0.20 \le Q_4^{\mathrm{G}} \le 0.20,\\
&-30.0^\circ \le \varphi_{34} \le 30.0^\circ,\\
&0.95 \le T_{35} \le 1.05,\\
&0.95 \le V_i \le 1.05, \quad i \in \{2,3,4,5\},\\
&-180.0^\circ \le \delta_i \le 180.0^\circ, \quad i \in \{2,3,4,5\}.
\end{aligned}$$

Voltage angles δ_1, δ_2, δ_3, and δ_4 are restricted to one full sweep of the unit circle. Slack bus generator powers P_1^{G} and Q_1^{G} are unrestricted, and branch current limits are neglected.

For this formulation, the vector of control variables is

$$u = \left(P_1^{\mathrm{G}}, P_3^{\mathrm{G}}, P_4^{\mathrm{G}}, Q_1^{\mathrm{G}}, Q_3^{\mathrm{G}}, Q_4^{\mathrm{G}}, \varphi_{34}, T_{35}\right)$$

and the vector of state variables is

$$x = (\delta_2, \delta_3, \delta_4, \delta_5, V_2, V_3, V_4, V_5).$$

The optimal solution for this formulation is

$$\begin{aligned}
&V_2 \approx 0.981, && V_3 \approx 0.957, && V_4 \approx 0.968, && V_5 \approx 0.959,\\
&\delta_2 \approx -12.59^\circ, && \delta_3 \approx -1.67^\circ, && \delta_4 \approx -13.86^\circ, && \delta_5 \approx -9.13^\circ,\\
&P_1^{\mathrm{G}} \approx 0.947, && P_3^{\mathrm{G}} \approx 0.192, && P_4^{\mathrm{G}} \approx 0.053,\\
&Q_1^{\mathrm{G}} \approx 0.387, && Q_3^{\mathrm{G}} \approx -0.127, && Q_4^{\mathrm{G}} \approx 0.200,\\
&\varphi_{34} \approx 12.38^\circ, && T_{35} \approx 0.95,
\end{aligned}$$

with objective function value 0.4016596*. If the controllable phase-shifting and tap-changing transformers are instead fixed to $\varphi_{34} = -3.0^\circ$ and $T_{35} = 0.98$, the optimal solution becomes*

$$\begin{aligned}
&V_2 \approx 0.983, && V_3 \approx 0.964, && V_4 \approx 0.970, && V_5 \approx 0.950,\\
&\delta_2 \approx -7.50^\circ, && \delta_3 \approx -4.22^\circ, && \delta_4 \approx -8.20^\circ, && \delta_5 \approx -8.64^\circ,\\
&P_1^{\mathrm{G}} \approx 0.946, && P_3^{\mathrm{G}} \approx 0.195, && P_4^{\mathrm{G}} \approx 0.058,\\
&Q_1^{\mathrm{G}} \approx 0.249, && Q_3^{\mathrm{G}} \approx -0.072, && Q_4^{\mathrm{G}} \approx 0.200,
\end{aligned}$$

with objective function value 0.4041438*, a cost increase of approximately 0.6%.* □

To obtain the optimal solution for Example 5.2, we implemented three versions of the classical formulation (5.1)–(5.9) in the GAMS modeling language. The three versions each use a different form of the power flow equations: (i) polar voltage coordinates with rectangular admittance coordinates (4.15)–(4.16), (ii) polar voltage coordinates with polar admittance coordinates (4.17)–(4.18), and (iii) rectangular voltage coordinates with rectangular admittance coordinates (4.19)–(4.20). The model is publicly available in the GAMS model library [1].[5] For the example, the model yielded

[5]Note to the reviewer: the GAMS model is attached at the end of the article. The model is not yet available for download in the GAMS model library as stated here, but will be finalized and made available when this paper is published.

identical optimal solutions using three local nonlinear solvers, SNOPT, MINOS, and CONOPT, and verified as globally optimal using the global solver LINDOGlobal.

5.2. Special Applications. Besides the classical ED formulation, several other OPF variants are common in both industry and research. These include security-constrained economic dispatch (SCED), security-constrained unit commitment (SCUC), optimal reactive power flow (ORPF), and reactive power planning (RPP).

5.2.1. Security-Constrained Economic Dispatch. Security-constrained economic dispatch (SCED), sometimes referred to as security-contrained optimal power flow (SCOPF), is an OPF formulation which includes power system contingency constraints [4]. A contingency is defined as an event which removes one or more generators or transmission lines from the power system, increasing the stress on the remaining network. SCED seeks an optimal solution that remains feasible under any of a pre-specified set of likely contingency events.

SCED formulations typically have the same objective function and decision variables u as the classic formulation.[6] However, they introduce N_C additional sets of state variables x and accompanying sets of power flow constraints, where N_C is the number of contingencies. SCED can be expressed in a general way as

$$\begin{aligned}
\min \quad & f(u, x_0), \\
\text{s.t.} \quad & g_0(u, x_0) = 0, \\
& h_0(u, x_0) \leq 0, \\
& g_c(u, x_c) = 0 \qquad \forall\ c \in \mathbf{C}, \\
& h_c(u, x_c) \leq 0 \qquad \forall\ c \in \mathbf{C},
\end{aligned} \tag{5.12}$$

where $\mathbf{C} = \{1, \ldots, N_C\}$ is the set of contingencies to consider. Each contingency has a distinct admittance matrix $\widetilde{Y}_c$ with less connectivity than the original system. Apart from the contingency index, f, g, and h are defined as the objective function, equality contstraints, and inequality constraints in the classical OPF formulation of §5.1, respectively. In other words, for each contingency $c \in \mathbf{C}$, the post-contigency power flow must remain feasible for the original decision variables u:

(i) The power flow equations must have a solution,
(ii) The contingency state variables x_c must remain within limits, and
(iii) Any inequality constraints, such as branch flow limits, must be satisfied.

Remark 5.3. Typically, the limits on the contingency-dependent state variables x_c and other functional inequality constraints are relaxed for the contingency cases compared to the base case. For example, system voltages are allowed to dip further during an emergency than under normal operating conditions. The relaxation of system limits is justified because operation under a contingency is temporary: when a contingency occurs, operators immediately begin re-configuring the system to return all branches and buses to normal operating limits.

SCED is a restriction of the classic OPF formulation: for the same objective function, the optimal solution to SCED will be no better than the optimal solution without considering contingencies. The justification for the restriction is that SCED mitigates the risk of a system failure (blackout) should one of the contingencies occur.

SCED has interesting connections to other areas of optimization. The motivation for SCED is theoretically similar to that of Robust Optimization (RO) [6], although

[6] In SCED, the slack bus real and reactive power are treated as state variables because they must be allowed to change for each contingency in order for the system to remain feasible.

RO typically addresses continuous uncertain parameters rather than discrete scenarios. Additionally, because the constraints are separable for a fixed u, SCED lends itself well to parallelization and decomposition algorithms [23].

5.2.2. Security-Constrained Unit Commitment. In electric power systems operation, unit commitment (UC) refers to the scheduling of generating units such that total operating cost is minimized. UC differs from ED in that it operates across multiple time periods and schedules the on-off status of each generator in addition to its power output. UC must address generator startup and shutdown time and costs, limits on generator cycling, ramp rate limits, reserve margin requirements, and other scheduling constraints. UC is a large-scale, multi-period, mixed-integer nonlinear programming (MINLP) problem. Many UC formulations relax certain aspects of the problem in order to obtain a mixed-integer linear program (MILP) instead—for instance by using linearized cost functions.

If the power flow equations are added to the UC problem, the formulation becomes security-constrained unit commitment (SCUC). In SCUC, a power flow is applied at each time period to ensure that the scheduled generation satisfies not only the scheduling constraints but also system voltage and branch flow limits. In other words, SCUC ensures that the UC algorithm produces a generation schedule that can be physically realized in the power system. Because of its complexity, research on SCUC has accelerated only with the advent of faster computing capabilities.

In SCUC, we introduce a time index $t \in \mathbf{T}$ and a set of binary control variables w_{it} to the OPF formulation. Each w_{it} indicates whether or not generator i is committed for time period t. The modified formulation becomes

$$
\begin{aligned}
\min \quad & \sum_{t\in\mathbf{T}}\sum_{i\in\mathbf{G}} \Big(w_{it} C_i\left(P_{it}^{\mathrm{G}}\right) + C_i^{\mathrm{SU}} w_{it}\left(1 - w_{i,t-1}\right) \\
& \qquad\qquad + C_i^{\mathrm{SD}}\left(1 - w_{it}\right) w_{i,t-1}\Big), && (5.13)\\
\text{s.t.} \quad & P_{it}\left(V_t,\delta_t\right) = P_{it}^{\mathrm{G}} - P_{it}^{\mathrm{L}} & \forall\, i\in\mathbf{N}, \forall\, t\in\mathbf{T}, \quad & (5.14)\\
& Q_{it}\left(V_t,\delta_t\right) = Q_{it}^{\mathrm{G}} - Q_{it}^{\mathrm{L}} & \forall\, i\in\mathbf{N}, \forall\, t\in\mathbf{T}, \quad & (5.15)\\
& w_{it}P_i^{\mathrm{G,min}} \le P_{it}^{\mathrm{G}} \le w_{it}P_i^{\mathrm{G,max}} & \forall\, i\in\mathbf{G}, \forall\, t\in\mathbf{T}, \quad & (5.16)\\
& w_{it}Q_i^{\mathrm{G,min}} \le Q_{it}^{\mathrm{G}} \le w_{it}Q_i^{\mathrm{G,max}} & \forall\, i\in\mathbf{G}, \forall\, t\in\mathbf{T}, \quad & (5.17)\\
& V_i^{\min} \le V_{it} \le V_i^{\max} & \forall\, i\in\mathbf{N}, \forall\, t\in\mathbf{T}, \quad & (5.18)\\
& \delta_i^{\min} \le \delta_{it} \le \delta_i^{\max} & \forall\, i\in\mathbf{N}, \forall\, t\in\mathbf{T}, \quad & (5.19)\\
& \varphi_{ik}^{\min} \le \varphi_{ikt} \le \varphi_{ik}^{\max} & \forall\, ik\in\mathbf{H}, \forall\, t\in\mathbf{T}, \quad & (5.20)\\
& T_{ik}^{\min} \le T_{ikt} \le T_{ik}^{\max} & \forall\, ik\in\mathbf{K}, \forall\, t\in\mathbf{T}, \quad & (5.21)\\
& I_{ikt}\left(V_t,\delta_t\right) \le I_{ik}^{\max} & \forall\, ik\in\mathbf{L}, \forall\, t\in\mathbf{T}, \quad & (5.22)\\
& P_i^{\mathrm{Down}} \le P_{it}^{\mathrm{G}} - P_{i,t-1}^{\mathrm{G}} \le P_i^{\mathrm{Up}} & \forall\, i\in\mathbf{G}, \forall\, t\in\mathbf{T}, \quad & (5.23)\\
& \sum_{i\in\mathbf{G}} w_{it}P_i^{\mathrm{G,max}} - \sum_{i\in\mathbf{G}} P_{it}^{\mathrm{G}} \ge P_{\mathrm{Reserve}} & \forall\, t\in\mathbf{T}. \quad & (5.24)
\end{aligned}
$$

The objective function (5.13) includes terms for unit startup costs C^{SU} and shutdown costs C^{SD} in addition to the generation costs in each time period. The generation limits (5.16)–(5.17) are modified such that uncommitted units must have zero real and reactive power generation. Current limit constraint (5.22) is a compact expression of (5.11) with an added time index. Constraint (5.23) specifies positive and negative generator ramp limits P^{Up} and P^{Down}, respectively; these are physical limitations of the generators. Constraint (5.24) requires a spinning reserve margin of at least P_{Reserve}; sometimes this constraint is written such that P_{Reserve} is a fraction of the total load in each time period.

The SCUC formulation (5.13)–(5.24) is one of many possible formulations. Some formulations include more precise ramp limits and startup and shutdown characteristics; others include constraints governing generator minimum uptime and downtime. Because of the scale and presence of binary decision variables, SCUC is one of the most difficult power systems optimization problems. Zhu [37, ch. 7] and Bai and Wei [5] provide more discussion of SCUC, including detailed formulations.

5.2.3. Optimal Reactive Power Flow. Optimal reactive power flow (ORPF), also known as reactive power dispatch or VAR control, seeks to optimize the system reactive power generation in order to minimize the total system losses. In ORPF, the system real power generation is determined a priori, from the outcome of (for example) a DC OPF algorithm, UC, or other form of ED. A basic ORPF formulation is

$$\begin{aligned}
\min\quad & P_1, && && (5.25)\\
\text{s.t.}\quad & P_i(V,\delta) = P_i^{\text{G}} - P_i^{\text{L}} && \forall\, i \in \mathbf{N}, && (5.26)\\
& Q_i(V,\delta) = Q_i^{\text{G}} - Q_i^{\text{L}} && \forall\, i \in \mathbf{N}, && (5.27)\\
& Q_i^{\text{G,min}} \le Q_i^{\text{G}} \le Q_i^{\text{G,max}} && \forall\, i \in \mathbf{G}, && (5.28)\\
& V_i^{\min} \le V_i \le V_i^{\max} && \forall\, i \in \mathbf{N}, && (5.29)\\
& \delta_i^{\min} \le \delta_i \le \delta_i^{\max} && \forall\, i \in \mathbf{N}, && (5.30)\\
& \varphi_{ik}^{\min} \le \varphi_{ik} \le \varphi_{ik}^{\max} && \forall\, ik \in \mathbf{H}, && (5.31)\\
& T_{ik}^{\min} \le T_{ik} \le T_{ik}^{\max} && \forall\, ik \in \mathbf{K}, && (5.32)\\
& I_{ik}(V,\delta) \le I_{ik}^{\max} && \forall\, ik \in \mathbf{L}. && (5.33)
\end{aligned}$$

The vector of control variables is

$$u = \left(P_1, Q^{\text{G}}_{i:i\in\mathbf{G}}, \varphi_{ik:ik\in\mathbf{H}}, T_{ik:ik\in\mathbf{K}}\right),$$

while the vector of state variables $x = (\delta, V)$ is identical to the classical formulation. In ORPF, all real power load and generation is fixed except for the real power at the slack bus, P_1. Minimizing P_1 is therefore equivalent to minimizing total system loss.

One motivation for using ORPF is the reduction of the variable space compared to fully coupled OPF [9]; another is the ability to reschedule reactive power to optimally respond to changes in the system load without changing the system real power setpoints. Many interior point algorithms for OPF have focused specifically on ORPF [11]. Zhu [37, ch. 10] discusses several approximate ORPF formulations and their solution methods.

5.2.4. Reactive Power Planning. Reactive power planning (RPP) extends the ORPF problem to the optimal allocation of new reactive power sources—such as capacitor banks—within a power system in order to minimize either system losses or total costs. RPP modifies ORPF to include a set of possible new reactive power sources; the presence or absence of each new source is modeled with a binary variable. The combinatorial nature of installing new reactive power sources has inspired many papers which apply heuristic methods to RPP [12].

A basic RPP formulation which minimizes total costs is

$$
\begin{aligned}
\min \quad & C_1\left(P_1\right)+\sum_{i \in \mathbf{Q}} w_i C_i^{\text{Install}}, && && (5.34)\\
\text{s.t.} \quad & P_i\left(V, \delta\right)=P_i^{\mathrm{G}}-P_i^{\mathrm{L}} && \forall\, i \in \mathbf{N}, && (5.35)\\
& Q_i\left(V, \delta\right)=Q_i^{\mathrm{G}}+Q_i^{\text{New}}-Q_i^{\mathrm{L}} && \forall\, i \in \mathbf{N}, && (5.36)\\
& Q_i^{\mathrm{G},\min} \leq Q_i^{\mathrm{G}} \leq Q_i^{\mathrm{G},\max} && \forall\, i \in \mathbf{G}, && (5.37)\\
& w_i Q_i^{\text{New},\min} \leq Q_i^{\text{New}} \leq w_i Q_i^{\text{New},\max} && \forall\, i \in \mathbf{Q}, && (5.38)\\
& V_i^{\min} \leq V_i \leq V_i^{\max} && \forall\, i \in \mathbf{N}, && (5.39)\\
& \delta_i^{\min} \leq \delta_i \leq \delta_i^{\max} && \forall\, i \in \mathbf{N}, && (5.40)\\
& \varphi_{ik}^{\min} \leq \varphi_{ik} \leq \varphi_{ik}^{\max} && \forall\, ik \in \mathbf{H}, && (5.41)\\
& T_{ik}^{\min} \leq T_{ik} \leq T_{ik}^{\max} && \forall\, ik \in \mathbf{K}, && (5.42)\\
& I_{ik}\left(V, \delta\right) \leq I_{ik}^{\max} && \forall\, ik \in \mathbf{L}. && (5.43)
\end{aligned}
$$

where C_i^{Install} represents the capital cost of each new reactive power source $i \in \mathbf{Q}$; Q_i^{New} is the amount of reactive power provided by each new reactive power source, subject to limits $Q_i^{\text{New},\min}$ and $Q_i^{\text{New},\max}$; and w_i is a binary variable governing the decision to install each new reactive power source. The modified vector of control variables is

$$u=\left(P_1, Q_{i:i \in \mathbf{G}}^{\mathrm{G}}, w_{i:i \in \mathbf{Q}}, Q_{i:i \in \mathbf{Q}}^{\text{New}}, \varphi_{ik:ik \in \mathbf{H}}, T_{ik:ik \in \mathbf{K}}\right). \tag{5.44}$$

Some variants of RPP also include real power dispatch in the decision variables or include multiple load scenarios.

By necessity, RPP optimizes with respect to uncertain future conditions—typically reactive power requirements for worst-case scenarios. This uncertainty, together with the problem complexity, make RPP a very challenging optimization problem [34]. Zhang et al. [34, 35] review both formulations and solution techniques for RPP.

6. Data Exchange.

Two common formats for the exchange of power flow and OPF case data are the IEEE Common Data Format [33] and the MATPOWER Case Format [38]. A number of publicly available test cases for OPF are distributed in one or both of these two formats [2, 38]. This section summarizes the structure of these formats and their relationship to the classical OPF formulation; the goal is to assist the reader in interpreting and applying available published data.

6.1. The IEEE Common Data Format.

The IEEE Common Data Format (CDF) was first developed in order to standardize the exchange of PF case data among utilities [33]. It has since been used to archive and exchange power systems test case data for the purpose of testing conventional PF and OPF algorithms. The format includes sections, or "cards",[7] for title data, bus data, branch data, loss zone data, and interchange data. Only the title, bus, and branch data are relevant for classical OPF as described in this primer. The full specification for the IEEE CDF can be found in [33] and an abbreviated description is available at [2].

Each IEEE CDF data card consists of plain text with fields delimited by character column. The title data card is a single line which includes summary information for

[7] Originally, the CDF data was exchanged among utilities by mail on paper card media.

TABLE 6.1

Field specification for IEEE Commmon Data Format bus data. The sixth column maps the field to an index, parameter, or variable used in the classical OPF formulation given in §5.1. (Some fields are used indirectly via inclusion in $\widetilde{Y}$.)

Field	Columns	Field Name	Data Type	Units	Quantity in OPF
1	1–4	Bus Number	Integer		i (bus index)
2	6–17	Bus Name	Text		
3	19–20	Bus Area	Integer		
4	21–23	Loss Zone Number[a]	Integer		
5	26	Bus Type	Integer		Special[b]
6	28–33	Voltage Magnitude	Numeric	p.u.	V_i
7	34–40	Voltage Angle	Numeric	deg.	δ_i
8	41–49	Load Real Power	Numeric	MW	P_i^{L}
9	50–58	Load Reactive Power	Numeric	MVAR	Q_i^{L}
10	59–67	Gen. Real Power	Numeric	MW	P_i^{G}
11	68–75	Gen. Reactive Power	Numeric	MVAR	Q_i^{G}
12	77–83	Base Voltage[a]	Numeric	kV	
13	85–90	Desired Voltage	Numeric	p.u.	V_i (Special[c])
14	91–98	Max. Reactive Power	Numeric	MVAR	$Q_i^{\mathrm{G,max}}$
		or			
		Max. Voltage Magnitude[d]	Numeric	p.u.	$V_i^{\max}$
15	99–106	Min. Reactive Power	Numeric	MVAR	$Q_i^{\mathrm{G,min}}$
		or			
		Min. Voltage Magnitude[d]	Numeric	p.u.	$V_i^{\min}$
16	107–114	Bus Shunt Conductance	Numeric	p.u.	g_i^{S}
17	115–122	Bus Shunt Susceptance	Numeric	p.u.	b_i^{S}
18	124–127	Remote Bus Number	Integer		

[a]Optional field

[b]0=PQ, 1=PQ (within voltage limits), 2=PV (within VAR limits), 3=Swing

[c]Indicates target voltage magnitude for voltage-controlled (PV) buses

[d]Gives reactive power limits if bus type is 2, voltage limits if bus type is 1

the case, including the power base S_{Base} in MVA. The bus and branch data cards follow, beginning with the characters `BUS DATA FOLLOWS` and `BRANCH DATA FOLLOWS`, respectively, and ending with the flag characters `-999`. Each line within the card gives the data for a single bus or branch.

Tables 6.1 and 6.2 list the IEEE CDF field specifications for bus and branch data, respectively. The fields include a mixture of SI and per-unit quantities. Conversion of all quantities to per-unit is required prior to use in an OPF formulation. Nominal-valued and unused fields in the data have zero entries. This quirk of the specification requires some caution in processing the data; for example, a value of 0.0 in the branch voltage ratio field should be interpreted as a nominal tap ratio ($T = 1.0$).

The IEEE CDF format is adapted for the compact exchange of system control data rather than OPF data. The field structure therefore has several limitations:

1. Some IEEE CDF fields specify final variable values (for instance, voltages V_i) for conventional power flow. For OPF, these fields should be understood as a feasible or near feasible starting point rather than an optimal solution. (Due to rounding, the reported solution may not be strictly feasible.)

2. The fields bus type (bus field 5) and branch type (branch field 6) specify system control methods, and are therefore of limited use in OPF. However, the bus

Table 6.2

Field specification for IEEE Commmon Data Format branch data. The sixth column maps the field to an index, parameter, or variable used in the classical OPF formulation given in §5.1. (Some fields are used indirectly via inclusion in $\widetilde{Y}$.)

Field	Columns	Field Name	Data Type	Units	Quantity in OPF
1	1–4	Tap Bus Number	Integer		i (from bus index)
2	6–9	Z Bus Number	Integer		k (to bus index)
3	11–12	Line Area[a]	Integer		
4	13–15	Loss Zone Number[a]	Integer		
5	17	Circuit Number	Integer		
6	19	Branch Type	Integer		Special[b]
7	20–29	Branch Resistance	Numeric	p.u.	R_{ik}
8	30–39	Branch Reactance	Numeric	p.u.	X_{ik}
9	41–49	Branch Shunt Susceptance	Numeric	p.u.	b_{ik}^{Sh}
10	51–55	Line Rating 1[a]	Numeric	MVA	$I_{ik}^{\max}$ [c]
11	57–61	Line Rating 2[a]	Numeric	MVA	
12	63–67	Line Rating 3[a]	Numeric	MVA	
13	69–72	Control Bus Number	Integer		
14	74	Side	Integer		
15	77–82	Voltage Ratio	Numeric	p.u.	T_{ik}
16	84–90	Phase Angle	Numeric	deg.	φ_{ik}
17	91–97	Min. Voltage Tap	Numeric	p.u.	$T_{ik}^{\min}$
		or			
		Min. Phase Angle[d]	Numeric	deg.	$\varphi_{ik}^{\min}$
18	98–104	Max. Voltage Tap	Numeric	p.u.	$T_{ik}^{\max}$
		or			
		Max. Phase Angle[d]	Numeric	deg.	$\varphi_{ik}^{\max}$
19	105–111	Tap Step Size	Numeric	p.u.	
		or			
		Phase Angle Step Size[d]	Numeric	deg.	
20	113–119	Min. Voltage	Numeric	p.u.	
		or			
		Min. MVar Transfer	Numeric	MVar	
		or			
		Min. MW Transfer[e]	Numeric	MW	
21	120–126	Max. Voltage	Numeric	p.u.	
		or			
		Max. MVar Transfer	Numeric	MVar	
		or			
		Max. MW Transfer[e]	Numeric	MW	

[a] Optional field

[b] 0=Transmission line, 1=Fixed T and φ, 2=Controllable T and fixed φ (voltage control), 3=Controllable T and fixed φ (MVAR control), 4=Fixed T and controllable φ

[c] Conversion to per-unit current (using rated branch voltage) is required

[d] Gives voltage tap limits or step if branch type is 2 or 3, phase angle limits or step if branch type is 4

[e] Gives voltage limits if branch type is 2, MVAR limits if branch type is 3, MW limits if branch type is 4

and branch types govern the interpretation of certain other fields in the IEEE CDF, as described in the table footnotes. For example, for PQ buses, bus fields 14 and 15 give voltage limits $V_i^{\max}$ and $V_i^{\min}$, respectively. For PV buses, these same fields instead give reactive power generation limits $Q_i^{\mathrm{G},\max}$ and $Q_i^{\mathrm{G},\min}$, respectively.

3. For IEEE CDF fields which depend on the bus and branch types, the data are sufficient for conventional PF but incomplete for OPF. For example, the IEEE CDF lacks voltage limits for PV buses and reactive power generation limits at PQ buses; the field structure prevents these data from being available. The user must supply (or assume) values for the incomplete data.

4. The IEEE CDF lacks other data required for OPF, including generator real power limits and cost data.

Given these limitations, publicly archived IEEE CDF case data is most useful for obtaining the network structure and associated bus and branch admittance data.

6.2. MATPOWER Case Format. MATPOWER [39] is an open-source software package for MATLAB[8] including functions for both conventional PF and OPF. The MATPOWER case format is a set of standard matrix structures used to store power systems case data and closely resembles the IEEE CDF. The format is described in detail in the MATPOWER manual [38].

MATPOWER case data consists of a MATLAB structure with fields `baseMVA`, `bus`, `branch`, `gen`, and `gencost`. `baseMVA` is a scalar giving the system power base S_{Base} in MVA. The remaining fields are matrices. Like the IEEE CDF, the MATPOWER case structure uses a mixture of SI and per-unit quantities and specifies nominal-valued branch tap ratios as 0 instead of 1.0.

Tables 6.3, 6.4, and 6.5 describe the `bus`, `branch`, and `gen` matrices. The `gencost` matrix has the same number of rows as the `gen` matrix, but the column structure provides a flexible description of the generator cost function. Column 1 specifies the type of cost model: 1 for piecewise linear or 2 for polynomial. Columns 2 and 3 give the generator startup and shutdown costs. The interpretation of column numbers 4 and greater depends on the type of cost model:

- For a piecewise linear cost model, column 4 specifies the number of coordinate pairs n of the form (P, C) that generate the piecewise linear cost function. The next $2n$ columns, beginning with column 5, give the coordinate pairs $(P_0, C_0), \ldots, (P_{n-1}, C_{n-1})$, in ascending order. The units of C are \$/hr and the units of P are MW.
- For a polynomial cost model, column 4 specifies the number n of polynomial cost coefficients. The next n columns, beginning with column 5, give the cost coefficients $C_{n-1}, \ldots, C_0$ in descending order. The corresponding polynomial cost model is $C_{n-1}P^{n-1} + \ldots + C_1 P + C_0$. The units are such that the cost evaluates to dollars \$/hr for power given in MW.

If `gencost` is included, then MATPOWER case data contains nearly all the information necessary to formulate the classical OPF problem as described in §5.1. However, MATPOWER makes no provision for including transformer tap ratios or phase shifting transformer angles in the set of decision variables; therefore, limits on these variables are not present in the data structure. The user must supply limits for these controls if they exist in the formulation.

7. Conclusion. In this primer, we have addressed the basic, practical aspects of Optimal Power Flow formulations. For the reader interested in learning more, particu-

[8]MATLAB is a popular technical computing environment produced by The MathWorks, Inc.

Table 6.3

Field specification for bus data matrix in MATPOWER case data (input fields only). The fifth column maps the field to an index, parameter, or variable used in the classical OPF formulation given in §5.1. (Some fields are used indirectly via inclusion in $\widetilde{Y}$.)

Column	Field Description	Data Type	Units	Quantity in OPF
1	Bus Number	Integer		i (bus index)
2	Bus Type	Integer		Special[a]
3	Load Real Power	Numeric	MW	P_i^{L}
4	Load Reactive Power	Numeric	MVAR	Q_i^{L}
5	Bus Area	Integer		
6	Bus Shunt Conductance	Numeric	MW[b]	g_i^{S}
7	Bus Shunt Susceptance	Numeric	MVAR[b]	b_i^{S}
8	Voltage Magnitude	Numeric	p.u.	V_i
9	Voltage Angle	Numeric	deg.	δ_i
10	Base Voltage	Numeric	kV	
11	Loss Zone	Integer		
12	Max. Voltage Magnitude	Numeric	p.u.	$V_i^{\max}$
13	Min. Voltage Magnitude	Numeric	p.u.	$V_i^{\min}$

[a]1=PV, 2=PQ, 3=Swing, 4=Isolated

[b]Specified as a MW or MVAR demand for $V = 1.0$ p.u.

Table 6.4

Field specification for branch data matrix in MATPOWER case data (input fields 1–11 only). The fifth column maps the field to an index, parameter, or variable used in the classical OPF formulation given in §5.1. (Some fields are used indirectly via inclusion in $\widetilde{Y}$.)

Column	Field Description	Data Type	Units	Quantity in OPF
1	Tap Bus Number	Integer		i (from bus index)
2	Z Bus Number	Integer		k (to bus index)
3	Branch Resistance	Numeric	p.u.	R_{ik}
4	Branch Reactance	Numeric	p.u.	X_{ik}
5	Branch Shunt Susceptance	Numeric	p.u.	b_{ik}^{Sh}
6	Line Rating (Long-term)	Numeric	MVA	$I_{ik}^{\max}$ [c]
7	Line Rating (Short-term)	Numeric	MVA	
8	Line Rating (Emergency)	Numeric	MVA	
9	Voltage Ratio	Numeric	p.u.	T_{ik}
10	Phase Angle	Numeric	deg.	φ_{ik}
11	Branch Status	Binary		

[a]Conversion to per-unit current (using rated branch voltage) is required

larly regarding optimization algorithms than have been used for OPF, we recommend any of the following:

1. Read the classical papers on OPF, for instance [4, 10, 27, 29]. These papers provide a detailed discussion of the foundations of OPF and provide context for more recent work.

2. Review textbooks which describe the OPF problem [32,37]. These textbooks provide clear, detailed formulations and also provide lists of relevant references.

3. Review the survey papers on OPF from the past several decades, for instance [11,12,17–19]. Reading the older surveys prior to the more recent ones provides insight into how OPF has developed over time.

4. Experiment with the GAMS OPF formulations provided to accompany Ex-

Table 6.5
Field specification for generator data matrix in MATPOWER case data (input fields 1–10 only). The fifth column maps the field to an index, parameter, or variable used in the classical OPF formulation given in §5.1.

Column	Field Description	Data Type	Units	Quantity in OPF
1	Bus Number	Integer		i (generator index)
2	Gen. Real Power	Numeric	MW	P_i^{G}
3	Gen. Reactive Power	Numeric	MVAR	Q_i^{G}
4	Max. Reactive Power	Numeric	MVAR	$Q_i^{\mathrm{G,max}}$
5	Min. Reactive Power	Numeric	MVAR	$Q_i^{\mathrm{G,min}}$
6	Voltage Setpoint	Numeric	p.u.	
7	Gen. MVA Base[a]	Numeric	MVA	
8	Generator Status[b]	Binary		
9	Max. Real Power	Numeric	MW	$P_i^{\mathrm{G,max}}$
10	Min. Real Power	Numeric	MW	$P_i^{\mathrm{G,min}}$

[a]Defaults to system power base S_{Base}
[b]0 indicates generator out of service (remove from OPF formulation)

ample 5.2, which are available in the GAMS model library [1]. Alternatively, install and experiment with the OPF capabilities available in MATPOWER [39]. Either software will provide insight into the practical challenges of OPF.

The material presented in this primer should provide a sufficient foundation for understanding the content of the references cited in this list.

In recent years, OPF has become one of the most widely researched topics in electric power systems engineering. We hope that this primer encourages a similar level of engagement within the Operations Research community, particularly in the development of new, efficient OPF algorithms.

Acknowledgment. We thank Kathryn Schumacher of the University of Michigan for her valuable comments and suggestions during the drafting of this primer.

REFERENCES

[1] *GAMS Model Library*. Internet site. Available: `http://gams.com/modlib/modlib.htm`.

[2] *Power Systems Test Case Archive*. Internet site. Available: `http://www.ee.washington.edu/research/pstca/`.

[3] O. Alsac, J. Bright, M. Praise, and B. Stott, *Further developments in LP-based optimal power flow*, IEEE Transactions on Power Systems, 5 (1990), pp. 697–711.

[4] O. Alsac and B. Stott, *Optimal load flow with steady-state security*, IEEE Transactions on Power Apparatus and Systems, PAS-93 (1974), pp. 745–751.

[5] X. Bai and H. Wei, *Semi-definite programming-based method for security-constrained unit commitment with operational and optimal power flow constraints*, IET Generation, Transmission & Distribution, 3 (2009), pp. 182–197.

[6] D. Bertsimas, D.B. Brown, and C. Caramanis, *Theory and applications of robust optimization*, SIAM Review, 53 (2011), pp. 464–501.

[7] R.C. Burchett, H.H. Happ, and K.A. Wirgau, *Large scale optimal power flow*, IEEE Transactions on Power Apparatus and Systems, 101 (1982), pp. 3722–3732.

[8] J. Carpentier, *Contribution to the economic dispatch problem*, Bulletin de la Société Française des Electriciens, 8 (1962), pp. 431–447.

[9] G.C. Contaxis, C. Delkis, and G. Korres, *Decoupled Optimal Load Flow Using Linear or Quadratic Programming*, IEEE Transactions on Power Systems, PWRS-I (1986), pp. 1–7.

[10] H.W. Dommel and W.F. Tinney, *Optimal power flow solutions*, IEEE Transactions on Power Apparatus and Systems, 87 (1968), pp. 1866–1876.

[11] S. Frank, I. Steponavice, and S. Rebennack, *Optimal Power Flow: A Bibliographic Survey I, Formulations and Deterministic Methods*, Energy Systems, tba (2012), p. tba.

[12] ———, *Optimal Power Flow: A Bibliographic Survey II, Non-Deterministic and Hybrid Methods*, Energy Systems, tba (2012), p. tba.

[13] Eberhard Freitag and Rolf Busam, *Complex Analysis*, Springer, 2 ed., 2009.

[14] J.D. Glover, M.S. Sarma, and T.J. Overbye, *Power System Analysis and Design*, Cengage Learning, Stamford, CT, 4 ed., 2008.

[15] S. Granville, *Optimal reactive dispatch through interior point method*, IEEE Transactions on Power Systems, 9 (1994), pp. 136–146.

[16] M. Greenberg, *Advanced Engineering Mathematics*, Prentice Hall, Upper Saddle River, NJ, 2 ed., 1998.

[17] M. Huneault and F.D. Galiana, *A survey of the optimal power flow literature*, IEEE Transactions on Power Systems, 6 (1991), pp. 762–770.

[18] J.A. Momoh, M.E. El-Hawary, and R. Adapa, *A Review of Selected Optimal Power Flow Literature to 1993 Part II: Newton, Linear Programming and Interior Point Methods*, IEEE Transactions on Power Systems, 14 (1999), pp. 105–111.

[19] J. A. Momoh, M.E. El-Hawary, and R. Adapa, *A Review of Selected Optimal Power Flow Literature to 1993 Part I: NonLinear and Quadratic Programming Approaches*, IEEE Transactions on Power Systems, 14 (1999), pp. 105–111.

[20] J. Nocedal and S. Wright, *Numerical Optimization*, Springer, New York, NY, 2nd ed., 2006.

[21] J. O'Malley, *Schaum's Outline of Basic Circuit Analysis*, Schaum's Outline Series, McGraw-Hill, New York, NY, 2 ed., 2011.

[22] J. Peschon, D.W. Bree, and L.P. Hajdu, *Optimal Power-Flow Solutions for Power System Planning*, Proceedings of the IEEE, 6 (1972), pp. 64–70.

[23] W. Qiu, A.J. Flueck, and F. Tu, *A new parallel algorithm for security constrained optimal power flow with a nonlinear interior point method*, in IEEE Power Engineering Society General Meeting, 2005, pp. 2422–2428.

[24] R.L. Rardin, *Optimization in Operations Research*, Prentice Hall, Upper Saddle River, NJ, 1 ed., 1997.

[25] N.S. Rau, *Issues in the path toward an RTO and standard markets*, IEEE Transactions on Power Systems, 18 (2003), pp. 435–443.

[26] ———, *Optimization Principles: Practical Applications to the Operation and Markets of the Electric Power Industry*, Wiley-IEEE Press, Hoboken, NJ, 2003.

[27] B. Stott and E. Hobson, *Power System Security Control Calculation Using Linear Programming Parts I and II*, IEEE Transactions on Power Apparatus and Systems, PAS-97 (1978), pp. 1713–1731.

[28] B. Stott, J. Jardim, and O. Alsac, *DC power flow revisited*, IEEE Transactions on Power Systems, 24 (2009), pp. 1290–1300.

[29] D.I. Sun, B. Ashley, B. Brewer, A. Hughes, and W.F. Tinney, *Optimal power flow by Newton approach*, IEEE Transactions on Power Apparatus and Systems, 103 (1984), pp. 2864–2880.

[30] G.L. Torres and V.H. Quintana, *An Interior-Point Method For Nonlinear Optimal Power Flow Using Voltage Rectangular Coordinates*, IEEE Transactions on Power Systems, 13 (1998), pp. 1211–1218.

[31] L.S. Vargas, V.H. Quintana, and A. Vannelli, *A tutorial description of an interior point method and its applications to security-constrained economic dispatch*, IEEE Transactions on Power Systems, 8 (1993), pp. 1315–1323.

[32] A.J. Wood and B.F. Wollenberg, *Power Generation, Operation, and Control*, John Wiley & Sons, Inc., New York, NY, 2 ed., 1996.

[33] Working Group on a Common Format for Exchange of Solved Load Flow Data, *Common Format For Exchange of Solved Load Flow Data*, IEEE Transactions on Power Apparatus and Systems, PAS-92 (1973), pp. 1916–1925.

[34] W. Zhang, F. Li, and L.M. Tolbert, *Review of Reactive Power Planning: Objectives, Constraints, and Algorithms*, IEEE Transactions on Power Systems, 22 (2007), pp. 2177–2186.

[35] W. Zhang and L.M. Tolbert, *Survey of Reactive Power Planning Methods*, in IEEE Power Engineering Society General Meeting, vol. 2, June 2-16 2005, pp. 1430–1440.

[36] X.-P. Zhang, *Fundamentals of Electric Power Systems*, John Wiley & Sons, Inc., 2010, ch. 1, pp. 1–52.

[37] J. Zhu, *Optimization Of Power System Operation*, Wiley-IEEE, Piscataway, NJ, 2009.

[38] R.D. Zimmerman and C.E. Murillo-Sánchez, *MATPOWER 4.1 User's Manual*, Power Systems Engineering Research Center (PSERC), 2011.

[39] R.D. Zimmerman, C.E. Murillo-Sánchez, and R.J. Thomas, *MATPOWER: Steady-State*

Operations, Planning, and Analysis Tools for Power Systems Research and Education, IEEE Transactions on Power Systems, 26 (2011), pp. 12–19.